INFORMATION TO USERS

This manuscript has been reproduced from the microfilm master. UMI films the text directly from the original or copy submitted. Thus, some thesis and dissertation copies are in typewriter face, while others may be from any type of computer printer.

The quality of this reproduction is dependent upon the quality of the copy submitted. Broken or indistinct print, colored or poor quality illustrations and photographs, print bleedthrough, substandard margins, and improper alignment can adversely affect reproduction.

In the unlikely event that the author did not send UMI a complete manuscript and there are missing pages, these will be noted. Also, if unauthorized copyright material had to be removed, a note will indicate the deletion.

Oversize materials (e.g., maps, drawings, charts) are reproduced by sectioning the original, beginning at the upper left-hand corner and continuing from left to right in equal sections with small overlaps. Each original is also photographed in one exposure and is included in reduced form at the back of the book.

Photographs included in the original manuscript have been reproduced xerographically in this copy. Higher quality 6" x 9" black and white photographic prints are available for any photographs or illustrations appearing in this copy for an additional charge. Contact UMI directly to order.

UMI

A Bell & Howell Information Company
300 North Zeeb Road, Ann Arbor MI 48106-1346 USA
313/761-4700 800/521-0600

MOLECULAR RECOGNITION IN THE
STREPTAVIDIN-BIOTIN SYSTEM

by

Vano Chu

A dissertation submitted in partial fulfillment of
the requirements for the degree of

Doctor of Philosophy

University of Washington

1998

Approved by 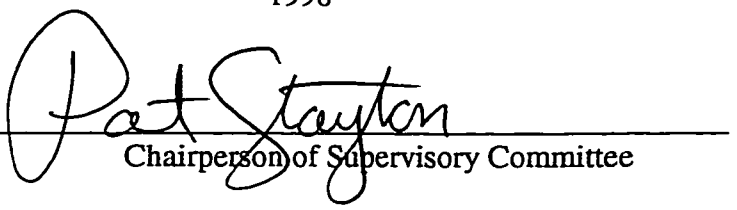
Chairperson of Supervisory Committee

Program Authorized
to Offer Degree Department of Bioengineering

Date December 15, 1998

Doctoral Dissertation

In presenting this dissertation in partial fulfillment of the requirements for the Doctoral degree at the University of Washington, I agree that the Library shall make its copies freely available for inspection. I further agree that extensive copying of this dissertation is allowable only for scholarly purposes, consistent with "fair use" as prescribed in the U.S. Copyright Law. Requests for copying or reproduction of this dissertation may be referred to University Microfilms, 1490 Eisenhower Place, P.O. Box 975, Ann Arbor, MI 48106, to whom the author has granted "the right to reproduce and sell (a) copies of the manuscript in microform and/or (b) printed copies of the manuscript made from microform."

Signature 

Date 12·15·98

University of Washington

Abstract

MOLECULAR RECOGNITION IN THE STREPTAVIDIN-BIOTIN SYSTEM

by Vano Chu

Chairperson of the Supervisory Committee: Professor Patrick Stayton
Department of Bioengineering

In this project, the bases for high-affinity interaction and ligand recognition were investigated in the streptavidin-biotin system. With an estimated binding constant on the order of 10^{13} M^{-1}, the binding of biotin to streptavidin is one of the strongest non-covalent interactions known. Here, we report the results of combined structural and thermodynamic efforts toward defining the contributions of two components of the tight-binding phenomenon—a flexible loop which closes over the binding site and a key residue in the hydrogen bond network to biotin. To probe the role of the loop, a new mutagenesis technique based on creating circularly permuted variants of core streptavidin was used to create discontinuities in the binding-site loop and to remove it entirely through relocation of the termini without changing the overall structure of the protein. The loop alterations result in drastic reductions in binding affinity accompanied by large increases in the dissociation rate of biotin from the binding site. The results of the flexible loop alterations underscore the magnitude of the contribution which loop closure provides to the stability of the streptavidin-biotin complex. Also, site-directed mutagenesis was used to remove a hydrogen bond from aspartate-128 to a ureido nitrogen of biotin by changing the residue to alanine (D128A). This modification also generated a large drop in affinity with a concomitant increase in dissociation rates. Parallel studies in x-ray crystallography and in molecular modeling provided the surprising finding that the structure of the D128A-biotin complex very closely resembles an intermediate structure seen in most of the computed dissociation pathways. The D128A-biotin complex may be viewed

essentially as a stable, structural snapshot of an intermediate state on the dissociation reaction coordinate.

TABLE OF CONTENTS

LIST OF FIGURES

LIST OF TABLES

LIST OF ABBREVIATIONS

ASA. Accessible surface area.

ΔASA Change in accessible surface area.

ΔC_p Change in molar heat capacity.

CPn/c. Circularly permuted streptavidin with new N-terminus at position n and new C-terminus at position c (using the original wild-type numbering system).

CP51/46 Circularly permuted streptavidin in which the loop is excised by creating termini at the loop edges.

CP50/49 Circularly permuted streptavidin in which the loop is nicked "downstream" of N49.

CP49/48 Circularly permuted streptavidin in which the loop is nicked "upstream" of N49.

D128A Streptavidin mutant in which Aspartate-128 has been changed to Alanine. The side chain of D128 normally hydrogen bonds to one of biotin's ureido nitrogens.

ITC. Isothermal titration calorimetry.

N49 Asparagine-49. A loop residue which hydrogen bonds to the biotin carboxylate in the bound complex of wild type.

WT. Wild type recombinant streptavidin, comprising residues 13–139 when expressed in *E. coli*.

ACKNOWLEDGEMENTS

The author wishes to acknowledge the assistance, guidance, and patience of his advisors: Professors Patrick Stayton and Christopher Viney. He would also like to thank Professor Ronald Stenkamp for assistance and moral support "above and beyond the call of duty" for a Ph.D. committee member. In addition, thanks go to all the unofficial teachers and mentors: Cyndi Long, Dr. Lisa Klumb, Dr. Philip Tan, and Dr. David Hyre.

The work reported here was supported by a generous fellowship from the Whitaker Foundation and by grants from the National Institutes of Health.

Thanks to all the folks from the Stayton and Vogel groups who made working in lab so enjoyable; to Stefanie Freitag and Isolde LeTrong for determining all those beautiful protein structures; to John Gilman, Bruce LeSourd, and Chris Ferris for their entropic contributions to my research; and to Aurora Graf for making me her high-affinity interaction of choice.

DEDICATION

The author wishes to dedicate this dissertation to his parents, But-Shee and Grace, for their enthusiastic and unwavering support of his academic endeavors.

CHAPTER 1: INTRODUCTION

MOLECULAR RECOGNITION

The machinery which has evolved over the millennia to sustain life includes a variety of proteins whose purpose is to pick out a particular ligand from the myriad of swarming molecules in the surrounding environment and to hang onto it. The result of this binding event may be modification of the ligand, triggering of a signaling cascade, or simple sequestration of the molecule. For many research groups, the puzzle lies in how said protein is able to recognize and retain a particular ligand above all others.

To dissect the components responsible for creating high-affinity interactions, the streptavidin-biotin system has been used by several research groups as a model system for investigating the origins of tight-binding phenomena.[1] Streptavidin is a tetrameric protein (MW~60000) that binds biotin (vitamin H) with an exceptionally high affinity for a noncovalent interaction—$K_a \sim 2.5 \cdot 10^{13}$.[2] Each subunit is an 8-stranded, antiparallel, β-sheet barrel structure that binds one 244 Dalton biotin molecule. The four subunits are distributed about three, two-fold symmetry axes such that the binding sites are located in pairs on opposite "sides" of the tetramer. Streptavidin, when first expressed in its natural state in *Streptomyces avidinii*, comprises 159 amino acids. Post-translational processing usually truncates the protein to 125–127 residues—a form termed "core" streptavidin which is more soluble but retains binding activity.[3] In the Stayton laboratory, a synthetic gene coding for 127 residues of "core" streptavidin (residues 13 through 139) and optimized for expression in *E. coli* was constructed by Chilkoti.[4] The protein synthesized from this gene is hereafter referred to in this document as "wild-type" (WT), and all mutant versions of streptavidin described in this project are derived from the WT gene.

The specific, tight-binding interaction of the streptavidin-biotin system enjoys extensive use in a variety of assays and separation schemes because conjugating biotin to another biomolecule can usually be done without affecting the function of the target.[5, 6] In addition, the robustness and versatility of the streptavidin-biotin system has encouraged further exploration of its utility in the areas of cancer therapy[7], stimuli-responsive polymers[8], and nanotechnology.[9] Thus, aside from the theoretical interest in understanding the determinants of high-affinity binding, many of the mutants of streptavidin produced in the course of research may find further application in biotechnology or medicine.

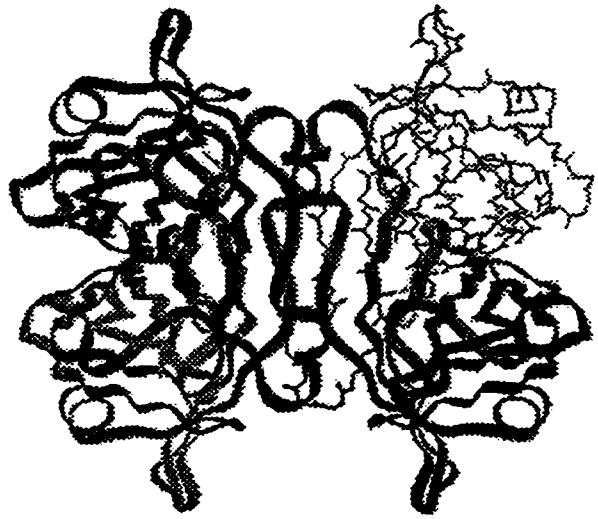

Figure 1. Streptavidin tetramer

Generation of the highly stable protein-ligand complex appears to depend on three main components of the streptavidin-biotin system:

- A number of tryptophan residues which surround the binding site. [4, 10, 11]
- An extensive hydrogen-bonding network to the ureido group elements and to the carboxylate of biotin.[12, 13]
- A flexible surface loop which closes over the binding site when biotin is present.[14, 15]

The X-ray structure of both bound and unbound streptavidin has been determined (Figure 1), yet surprisingly little is known about how these components combine to produce such a strong interaction. [13, 16-18] Investigations into the origins of the high-affinity in the streptavidin-biotin system would not only increase knowledge of ligand binding interactions, but also provide landmarks for directed manipulation of the binding characteristics of streptavidin itself and for rational design of drugs that act as protein ligands. One approach for studying the streptavidin-biotin complex is to perturb the system by changing the ligand or by changing the protein. A number of studies have been done on alternate ligands for streptavidin and in every case, the affinity for the new ligand is lower than that for biotin—sometimes by many orders of magnitude.[19-25] In contrast, the only groups who have reported mutagenesis studies on streptavidin have been our own laboratory and that of Cantor's group at Boston University.[26-28] Other approaches to investigating high-affinity binding are computer modeling of the system[29] and atomic force microscopy (AFM) experiments wherein the ligand is pulled from the site.[30, 31] There has also been a report in which computer modeling has been used to simulate the AFM experiments.[32] No clear picture has yet emerged on the roles of the components of the system. For example, there is still disagreement over whether the hydrogen-bonding network or the hydrophobic contacts are the main energetic contributors to the

interaction. What is clear is that mutations of just one residue in the protein can drastically reduce the affinity of streptavidin for biotin.

FLEXIBLE LOOPS

A large part of this document focuses on the role of the flexible loop which closes over biotin at the binding site. Flexible loops are often found near the binding or active sites of receptors and enzymes and in many cases, undergo a conformational change to a "closed" position upon ligand binding. Virtually all of the published reports on flexible loops describe enzyme-substrate systems rather than simple ligand binding (for a review, see Kempner[33]). In each case, the loop appears to have several possible roles:[34]

- Stabilization of an intermediate
- Steric retention of the substrate
- Exclusion of solvent to prevent competing reactions

In triosephosphate isomerase (TIM), the 11-residue binding site loop acts as a "lid" for the binding site. Since it has no catalytic residues itself, the loop appears to stabilize the enediol intermediate and prevent its loss into solution.[35-37] Though the crystal structure of TIM has been solved with a number of ligands[38, 39], there is still debate over the mechanism responsible for loop closure: At present, proposed mechanisms include long-range electrostatics[40], coupling to a deprotonation event[36], and natural motion of the protein on the 100-μs scale.[41]

The 13-residue flexible loop of lactate dehydrogenase also acts as a lid for the binding site. Its role appears to be polarization of the pyruvate substrate and stabilization of the intermediate. The mechanism for closure appears to be neutralization of positive charge repulsion between the loop and the binding site by the entry of the negatively charged

substrate.[42, 43] Other enzymes with "lids" at their active sites include adenylate kinase[44] and ribulose-1,5-bisphosphate carboxylase/oxygenase (Rubisco).[45]

Glutathione synthetase and dihydrofolate reductase both contain loops which are disordered in the unbound state (as opposed to the open "lids" on triosephosphate isomerase and lactate dehydrogenase) and which achieve an ordered, closed conformation on substrate binding. (This is what is believed to occur in the streptavidin-biotin system). In the enzymes, the loops are hypothesized to protect the intermediate from decomposition by water[46] and to stabilize the intermediate state.[47, 48] Tanaka *et al.* have also performed an experiment in which the glutathione synthetase loop was nicked by proteolysis.[49] They discovered that while catalytic activity was reduced, both halves of the loop appeared to independently close to protect the intermediate. In this document, I will report "nicking" of the streptavidin loop starting at the genetic level.

As biotin does not undergo any sort of chemical change after binding to streptavidin, the flexible loop of streptavidin must serve some other role. The loop presumably plays an important role in gating ligand association and dissociation, but their energetic contributions to molecular recognition remain unclear. The free energy of binding is a combination of several effects:

1. The enthalpic benefits of burying nonpolar surface area
2. The enthalpic benefits of establishing hydrogen-bond and electrostatic binding contacts
3. The entropic costs of ordering of loops
4. The entropic benefit of releasing bound water

These costs and benefits must be balanced to obtain optimal binding in the context of physiological function; higher affinity is not always desirable. In the binding of GroES to the GroEL chaperonin, it has been suggested that the ordering of the loop generates an entropy penalty in order to *reduce* the affinity of the interaction and make it

reversible via ATP hydrolysis.[50] As one approach to studying the energetic contributions, one might expect that protein/ligand interactions would have energetic signatures similar to those associated with protein folding.[51, 52]

Our group has recently reported a crystallographic study of the flexible loop in core streptavidin.[14] The loop (residues 45-52) is in a closed conformation in the presence of biotin and in an open conformation in unbound streptavidin (Figure 2). In our monoclinic crystal forms, residues 49 through 52 are found in a 3_{10} helix and the open conformation is stabilized by a hydrogen bonding interaction between residues 45 and 52. In a tetragonal crystal form, these residues are disordered in the open conformation.[13] Altogether, there are three hydrogen bonds to biotin mediated by residues near or in the loop: Ser45 terminates the β-strand leading into the loop and the side-chain oxygen of this residue is hydrogen-bonded to one of the ureido nitrogen atoms of biotin; the hydroxyl of Tyr43 donates a hydrogen bond to the ureido-oxygen of biotin; and the backbone amide nitrogen of Asn49 is hydrogen-bonded to the biotin carboxylate. My goal in this report is to further investigate the contributions of the flexible loop through mutagenesis of the loop itself.

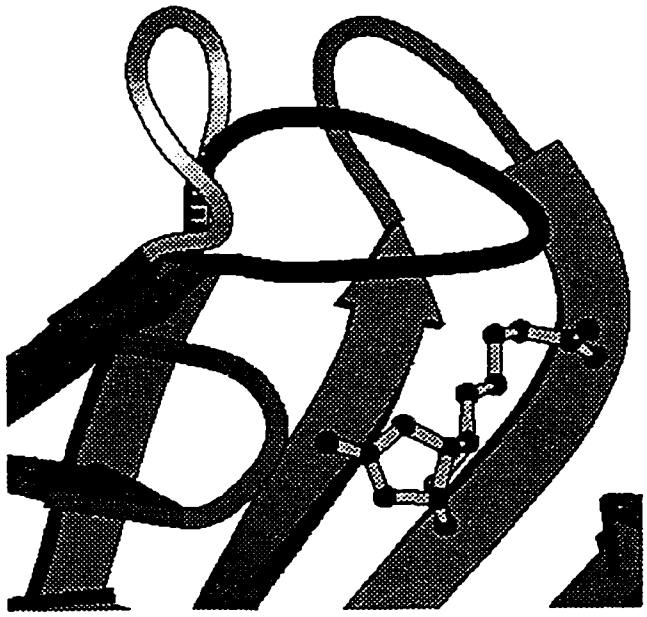

Figure 2. Streptavidin binding site loop. Closed position shown in black.

CIRCULAR PERMUTATION

In approximately one-third of the proteins for which structures are known, the proteins fold in such a way that the N- and C-termini lie in close proximity.[53] Conceivably, one could then ligate the termini and create a *circular* version of the protein. As a next step, one might then cut the protein once anywhere along the circularized chain to create new termini. This then, is the same result achieved using circular permutation through post-translational modification of the protein or alteration of the gene sequence itself.

Concanavalin A is the only protein known to undergo circular permutation by natural means.[54] It belongs to a family of carbohydrate-binding plant proteins called lectins and shares both sequence and structural homology to two other members of the group: favin and pea lectin.[55-59] Through a series of apparent enzymatic steps, the termini of concanvalin A are joined and the chain is reopened between residues 118 and 119. It

is interesting to note that the DNA sequence homology of Concanavalin A to other lectins is direct. Only the final amino acid sequence has circularly permuted homology indicating that the permutation does, in fact, occur post-translationally.

The pioneering work done in 1983 on bovine pancreatic trypsin inhibitor was also accomplished post-translationally by chemically linking the termini and cleaving the circularized protein with trypsin.[60] Both the circular and the permuted forms were found to refold to the native conformation after reduction of the intramolecular disulfide bonds. Shortly after, Luger, *et al.* created the first circularly-permuted protein at the genetic level using phosphoribosyl anthranilate (PRAI) and discovered that it too, refolded into a conformation nearly identical to the wild-type protein.[61] Since then, the number of circular permutations has been growing as researchers discover more proteins to which this treatment may successfully be applied. Some of the proteins for which CP versions exist are listed in Table 1 and a recent review has been published by Heinemann.[62]

Table 1. Circularly permuted proteins

1. Bovine pancreatic trypsin inhibitor[61]
2. Phosphoribosyl anthranilate[62, 64, 65]
3. Dihydrofolate reductase[66-68]
4. T4 lysozyme[69]
5. Interleukin 1β[70]
6. Aspartate transcarbamoylase[71-73]
7. Interleukin-4 toxin[74]
8. β-glucanase H[75]
9. Outer membrane protein A[76]
10. Gp120/HIV-1[77]
11. Glycerol-3-phosphate dehydrogenase[78]
12. α-spectrin SH3 domain[79]
13. β-lactamase[80]
14. γB crystallin[81]
15. Phosphoglycerate kinase[82]

CP versions of proteins are interesting since they provide insight into the folding process for proteins. The success of CP mutants is strong evidence that the N-terminus of many proteins does not need to fold first and provide the core around which the rest of the protein chain must fold as it is synthesized. In at least two cases, however, permuting the sequence does affect the rate of either translation[63] or assembly in the cell membrane.[64] Thus far, CP mutations have been successful if the new termini are formed at a surface loop, but proteins have refolded even when the new ends were created in hydrophobic pockets.[65] Although the permuted proteins closely resemble the wild-type originals, one difference which has been noted in some cases is that the permuted protein is thermodynamically less stable than the wild-type. In fact, the 108/107 permutation of *E. coli* dihydrofolate reductase does not refold without the addition of ligand.

Beyond the question of protein folding, circular permutation has been applied to provide other types of structural alterations. One application for circular permutation is the optimization of fusion proteins. Before, if one member of the fusion was interfering with the function of the other, the only alternatives were to switch the order, use longer linkers, or mutate one or both the proteins.[66] Using circular permutation, the termini of one or both of the proteins can simply be moved to a more convenient location for the junction which allows free access to the active sites of both members. Luger's group also demonstrated that it was possible to generate additional iterations of a repeatable domain via permutation: In this case, a repeat unit from the C-terminus of PRAI was duplicated ahead of the N-terminus to create a 10-fold βα-barrel from the native 8-fold.

In this document, I will describe yet another set of applications for circular permutation mutants—removal of a flexible loop without re-ligation of the cut site and genetic "nicking" of a protein chain. Both sets of mutants will be directed toward revealing the

energetic contributions of the binding-site loop to the interaction of streptavidin and biotin.

CHAPTER 2: MATERIALS AND METHODS

The following materials and methods were used extensively in the research described in this document. The procedures described in this chapter apply to all of the proteins used; procedures specific to a particular mutant are described later in the Materials and Methods sections of the respective chapters.

MOLECULAR BIOLOGY

All of the streptavidin mutants were derived from a synthetic gene for core streptavidin (WT) created in the Stayton laboratory which had been subcloned into the pUC18 plasmid.[4] To create a site-directed mutation, restriction enzymes were used to remove a segment of the original gene. A synthetic replacement cassette (Integrated DNA Technologies, Coralville, IA) containing the desired mutation was then ligated into the gap. The mutant pUC18 plasmids were transformed into a maintenance cell line—NovaBlue (Novagen, Madison, WI) or TOP10F' (Invitrogen, Carlsbad, CA)—and the cells were plated onto Luria-Bertani agar supplemented with 100 μg/mL ampicillin (LB/Amp agar). Colonies containing the mutant plasmid were identified by PCR colony screening and the integrity of the mutant streptavidin genes therein was verified by dye-terminated DNA sequencing. A verified copy of the mutant gene would then be subcloned into the pET-21a plasmid, which contains the strong T7 promoter, and transformed into BL21(DE3) cells (Novagen, Madison, WI) in preparation for protein synthesis.

PROTEIN SYNTHESIS AND PURIFICATION

BL21(DE3) cells containing the mutant pET-21a plasmids were plated on LB/Amp agar. A 50 mL overnight culture in LB media was grown from a single colony selected

from the plate. After washing and centrifugation steps to remove waste products and β-lactamase, the cells were resuspended and used to inoculate 5 L of 2×YT media. Cells were allowed to grow at 37°C with agitation until mid-log phase as determined by optical absorbance (A_{600} = 0.6–1.0). At that point, isopropyl-β-D-thiogalactoside (IPTG) was added to a final concentration of 1 mM to induce protein synthesis. Cells were allowed to grow for another 2–3 hours at 37°C and were then harvested by centrifugation.

Streptavidin and its mutants normally accumulate into densely packed masses called inclusion bodies when expressed in *E. coli* under control of the T7 promoter. In this form, the protein is non-functional, but the inclusion bodies are highly enriched in streptavidin so that the target protein is, to some degree, pre-purified while in the cell. To extract these inclusion bodies, harvested cells were lysed using sonication and the insoluble fractions were collected by centrifugation in a series of 5–6 cycles of sonication, centrifugation, and resuspension in a washing buffer: 50 mM Tris·HCl, 200 mM NaCl, 5 mM EDTA, 8% sucrose, 1 mM phenylmethylsulfonyl fluoride (PMSF), and 1% Triton X-100 (Triton is present in the first 3 washes only). The extracted inclusion bodies were solubilized overnight at 4°C in 50 mM Tris·HCl, 6M guanidine in preparation for refolding and purification. After centrifugation to remove particulates, the solubilized protein was refolded by dropwise dilution into a 50-fold volume of refolding buffer: 50 mM Tris·HCl, 100 mM NaCl, 5 mM EDTA, 0.1 mM PMSF, pH 7.5. Dilution was carried out at 4°C with continuous stirring and the protein solution was allowed to equilibrate overnight at 4°C.

Refolded protein was concentrated using a stirred ultrafiltration cell (Amicon, Beverly, MA) and the now-functional protein was purified by affinity chromatography over an iminobiotin-agarose column (Pierce, Rockford, IL) which takes advantage of the differential affinity of streptavidin for iminobiotin with changes in pH.[67] All of the mutants described in this study retained sufficient affinity for purification using this

method. Protein-containing fractions were pooled and exchanged into a storage buffer of 50 mM Na_2HPO_4, 100 mM NaCl at pH 7.0. Further exchanges into new buffers were accomplished using Slide-a-Lyzer dialysis cartridges (Pierce, Rockford, IL).

CHARACTERIZATION

COMPOSITION, CONCENTRATION, AND MOLECULAR WEIGHT

N-terminal sequencing was performed on an Applied Biosystems Model 477A Sequencer (Univ. of Washington, Pharmacology). SDS/PAGE analysis was done using precast Mini-Protean 10-20% gradient gels (Bio-Rad. Hercules, CA). Electrospray mass spectrometry was performed on a VG Quattro II Tandem Quadrupole Mass Spectrometer (Univ. of Washington, Medicinal Chemistry). Protein concentration was determined by absorption using an extinction coefficient (ε_{280}) of 34000 $M^{-1}cm^{-1}$ for the subunit.[68] Since no alterations to the tryptophan, tyrosine, phenylalanine, or cysteine content of streptavidin were made in any of the mutations, this value was used to determine the concentration for all of the mutant proteins.[69]

ISOTHERMAL TITRATION CALORIMETRY

Isothermal titration calorimetry (ITC) experiments were done using a Calorimetry Science Corporation 4200 Calorimeter (Provo, UT). Protein solutions of 30-40 μM concentration were titrated by the addition of 20 x 5 μL aliquots of 750 μM biotin dissolved in the same buffer as the protein. All ITC experiments were done in either phosphate (50 mM sodium phosphate, 100 mM NaCl, pH 7.0) or Tris (50 mM Tris·HCl, 100 mM NaCl, pH 7.0) buffers. Biotin stock solutions at 15 mM concentration were created using an electrobalance for weighing out biotin to 0.01 mg accuracies.

Integration of the injection peaks in the isotherm was accomplished using the proprietary Dataworks™ software supplied by Calorimetry Science Corporation with the instrument. Further analysis was performed using the Igor Pro software package (Wavemetrics, Lake Oswego, OR). The average heat of mixing for each injection, as determined from post-titration dilution peaks within each isotherm, was subtracted from the reaction heats before data analysis. Nonlinear, least-squares fitting of the data to an equation describing noncooperative binding allowed the number of binding sites (n), association constant (K_a), and binding enthalpy ($\Delta H°$) to be determined assuming one binding site per subunit.[70]

$$Q^2\left(\frac{K_a}{V\Delta H}\right)+Q(-1-P_T nK_a-K_a L_T)+(P_T V\Delta H nK_a L_T)=0$$

Q: Cumulative heat of reaction

V: Reaction volume

P_T: Total concentration of protein available for binding

L_T: Total concentration of injected ligand

By rewriting this equation as the solution for the quadratic in terms of the cumulative heat, Q, we may plot Q against the total ligand concentration, L_T, and fit the data using n, K_a, and $\Delta H°$ as fitting parameters.

Off-Rate Assay

The off-rate (k_{off}) of biotin from the mutants was determined using a radiometric competition assay originally reported by Piran and modified in our lab to take advantage of new ultrafiltration technology.[10, 71] In a sodium phosphate solution (50 mM NaH_2PO_4, 100 mM NaCl, pH 7.0), streptavidin at 50 nM concentration was pre-loaded with 10 nM tritiated biotin (^{3}H-biotin). At the beginning of the experiment, non-tritiated biotin was introduced into solution to a final concentration of 50 μM.

Sampling intervals were chosen so that each experiment would span 3 to 4 half-lives. The dissociated ^{3}H-biotin at each time point was immediately separated from the protein via centrifugation through Microcon-10 filters (Amicon, Beverly, MA) at 3.2°C in a microcentrifuge (Eppendorf, Beverly, MA) at maximum speed (14000 rpm). The total spin time including acceleration and deceleration of the rotor was 47 seconds. The amount of dissociated ^{3}H-biotin was determined by adding 30μL of the filtrate to 5mL EcoLume scintillation cocktail (ICN Pharmaceuticals, Costa Mesa, CA) and using an LS-7000 liquid scintillation counter (Beckman, Fullerton, CA) to measure the counts (1-minute collection times).

The dissociation rate for the release of biotin from streptavidin was calculated from a plot of the logarithm of the fraction of biotin bound versus time according to the integrated expression for a first-order reaction. Since the actual quantity measured in this experiment is the amount of dissociated biotin at each time point, the equation is rewritten as follows:

$$\ln X_{bound} = -k_{off}t$$

$$\ln\left(\frac{C_{full} - C_t}{C_{full} - C_0}\right) = -k_{off}t$$

C_{full}: the count for the original 10 nM ^{3}H-biotin solution (full scale)

C_t: the count of dissociated ^{3}H-biotin in the sample at each time point

C_0: the count of dissociated ^{3}H-biotin in the protein-biotin solution before the addition of non-tritiated biotin (baseline)

From the off-rate values at the several temperatures, the transition-state enthalpy, $\Delta H^{\ddagger}$, and entropy, $\Delta S^{\ddagger}$, may be determined from a fit of the Eyring equation:

$$k_{off} = \frac{k_B T}{h} \exp\left(\frac{-(\Delta H^{\ddagger} - T\Delta S^{\ddagger})}{RT}\right)$$

k_B: Boltzmann's constant

h: Planck's constant

R: Gas constant

EQUILIBRIUM COMPETITION ASSAY

A radiometric assay was developed by Klumb to measure the thermodynamic free energy alterations for the mutants relative to wild type.[12] Using a wild-type mutant with an additional six histidines (WT-Tag) to enable separation over nickel resin (Ni-NTA. Qiagen. Chatsworth, CA), the partitioning of ^{3}H-biotin between the two proteins can be determined at equilibrium after removal of WT-Tag. Control assays of wild-type versus WT-Tag indicate that the addition of the histidine tag does not change WT-Tag's affinity for biotin. A complete competition curve is generated by varying the concentration of a non-tagged mutant streptavidin of interest, keeping the concentrations of the WT-Tag and ^{3}H-biotin constant, and determining the amount of ^{3}H-biotin bound to the non-tagged streptavidin after equilibration. ^{3}H-biotin (21 μM, Amersham, Chicago, IL) was added to a final concentration of 20 nM to mixtures of the WT-Tag (50 nM) and the mutant in phosphate buffer, pH 7. Imidazole (20 mM) was added to minimize any non-specific adsorption of the mutant that might result from the presence of the two native histidines (H87 and H127) in each monomer. The proteins and ligand mixtures were equilibrated over several half-lives for the wild type streptavidin-biotin dissociation rate ($t_{1/2}$ is 4.5 hours at 37 °C) with typical incubation times of 24 hours at 37°C. After equilibration, the WT-Tag streptavidin was removed by batch incubation for 1 hour with 50 μl of a 50% slurry of washed Ni-NTA resin. The mixture was then cleared extensively via centrifugation. The supernatants were collected, boiled in 5% SDS to liberate bound ^{3}H-biotin, and assayed for radioactivity. Under these conditions, 98% of the WT-Tag streptavidin was removed from solution by the Ni-NTA resin and nonspecific binding of the mutant streptavidin to the resin varied between 2 - 5%. A negligible amount of ^{3}H-biotin, in the absence of

streptavidin, was found to bind to the Ni-NTA resin, and in the presence of protein the free ^{3}H-biotin was less than 3% of the total ligand concentration.

From the expressions for the equilibrium constants for mutant and WT-Tag binding to streptavidin and the mass balance equations, we may derive the following equation assuming that the concentration of ^{3}H-biotin is insignificant (this is verified in each experiment):

$$(R-1)[CL]^2 + (L_T + C_T + R(P_T - L_T))[CL] - L_T C_T = 0$$

R: ratio of competitor K_d to WT-Tag K_d

[CL]: concentration of competitor-biotin complex

L_T, C_T, P_T: total concentrations of biotin, competitor, and WT-Tag

As this has the form of a quadratic, we may rewrite it in the form of the equation that solves for [CL]. L_T and P_T are fixed. [CL] may be plotted against C_T with R as the sole fitting parameter:

$$[CL] = \frac{-(L_T + C_T + R(P_T - L_T)) \sqrt{(L_T + C_T + R(P_T - L_T)^2 - 4(R-1)L_T C_T}}{2(R-1)}$$

A non-linear least squares fit of the data is performed to determine the ratio of dissociation constants.

Differential Scanning Calorimetry

Samples for differential scanning calorimetry (DSC) were prepared in the same manner as those for ITC. Briefly, a 25–30 μM solution of the protein of interest in phosphate buffer was degassed and injected into the DSC sample chamber. The buffer without protein was injected into the reference cell. Both solutions were placed under 2.80 atmospheres of pressure and subjected to 2–3 heating/cooling cycles over the

temperature range of 0–110°C. The heating and cooling rate was 1°C/min. Data processing and extraction of the melting point were accomplished using the supplied software from Calorimetry Sciences Corporation.

CHAPTER 3: BINDING SITE LOOP DELETION

INTRODUCTION

By creating a circular permutation of streptavidin, we were able to excise the binding site loop to gauge its relative contribution to the creation of the high-affinity complex. Generation of circularly permuted proteins provides an experimental means of investigating the biophysical consequences of loop removal on ligand binding in ways not available using traditional deletion mutants. Circular permutation allows loop removal without re-ligation of the protein chain since the cut ends simply become the new N- and C-termini of the mutant.

Circularly permuted proteins have been used previously to investigate the protein folding problem, and naturally occurring circularly permuted proteins have been identified.[1, 60-62] Prior crystallographic studies have shown that circular permutation does not perturb the overall folding of many proteins. In nature, the structure of concanavalin A[58] is very similar to that of pea lectin [56] and favin[57] even though the amino acid sequences of these proteins are circularly permuted. Recent structural studies of five artificially permuted proteins—two variants of jellyroll proteins [72], two mutants of α-spectrin SH3 domains[73], and a circularly permuted β-lactamase[74]—have shown that the overall folding of these molecules is conserved when compared to the non-permuted proteins.

We have used circular permutation to remove the loop while leaving free N- and C-termini at the site of excision to provide insight into the energetic contribution of flexible loops to ligand association.

MATERIALS AND METHODS

GENE CONSTRUCTION

Δ47–50. *The description of the design and construction of this mutant is included for completeness: After the initial successful expression and purification of what appeared to be the correct deletion mutant, I was unable to correctly express and refold the protein again despite dozens of attempts over a period of two years. Perhaps my successor in this project will find the key to reclaiming this protein.* Δ47–50 is a conventional deletion mutant in that it involves simple removal of residues 47, 48, 49, and 50 from the wild-type streptavidin sequence. The resultant protein has a new connection from residue 46 to residue 51 in its backbone. The mutation was created by cassette replacement between the *KpnI* and *XbaI* sites of the wild-type streptavidin gene in the pUC18 cloning plasmid. The replacement cassette for Δ47-50 was designed to eliminate the *KpnI* site upon ligation to allow for quick restriction screening to distinguish mutant genes from those of the wild-type. After confirmation of the desired mutations by restriction screening and DNA sequencing, the Δ47-50 gene was transferred to the pET-21a plasmid for expression.

Tandem Gene. Following the example of Horlick, *et al*, I first designed a genetic construct to act as a template from which all circular permutations of streptavidin could be made via a single PCR mutagenesis step with a pair of the appropriate primers. The template is a tandem gene—a single gene that codes for a complete copy of streptavidin, followed by a linker sequence to join the old N- and C-termini, followed by yet another complete copy of streptavidin.[75]

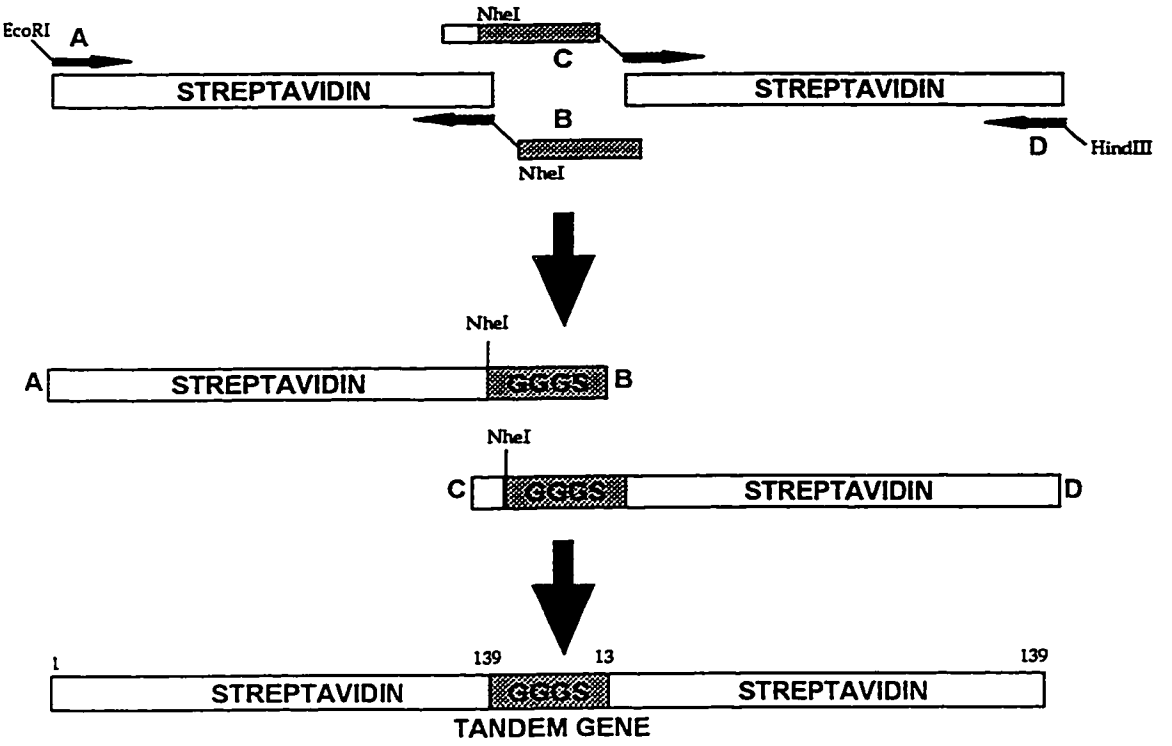

Figure 3. Tandem gene construction schematic

The gene was constructed in two halves from the wild-type streptavidin gene using PCR mutagenesis. Four primers (A, B, C, and D) were used pairwise to generate each half of the tandem gene. The first half (fragment AB) codes for the wild-type gene with a new linker sequence attached to the end. This linker sequence codes for an additional four amino acids, Gly-Gly-Gly-Ser, that act as a flexible bridge between the old N- and C-termini of streptavidin. The codons immediately preceding this linker sequence were modified to generate two unique restriction sites (*NheI* and *SacII*) without changing the amino acid sequence. The *NheI* restriction site would later be used to join the halves of the tandem gene. The second half (fragment CD) has the flexible linker, with its associated restriction sites, at the beginning of the gene instead of at the end. Both

fragments were generated in separate PCR mutagenesis reactions, ligated separately into pT7Blue plasmids, and transformed into HB101 cells. The DNA sequences of each set of fragments were checked against our expected sequences to confirm that no errors had been introduced during the PCR reaction. The CD fragment was excised using the *NheI* and *HindIII* restriction enzymes and inserted at the end of the AB fragment which was still in its pT7Blue plasmid. This completed construction of the tandem gene. It, too, was checked using DNA sequencing for errors.

CP51/46. The first permutation to be made from this template was designed to eliminate the central residues of the binding site flexible loop. Residues 46 and 51 were chosen to be the new termini because the penultimate residues, 45 and 52, were both serines that were hydrogen-bonded back to the main body of the protein in the X-ray structure. By having "anchors" just before the termini of the permuted protein chain, we hoped to keep the conformation of the backbone on either side of the missing loop as close as possible to that of the wild-type streptavidin.

To create a circular permutation from the tandem gene, a pair of new DNA primers had to be made. Primer 1 is designed to anneal starting at residue 51 of the AB fragment of the tandem gene and to add an *NdeI* site to the beginning of the final PCR product. The antisense primer, Primer 2, is designed to anneal at residue 46 of the CD fragment and to add stop codons and a *HindIII* site to the end of the product. PCR mutagenesis produces a fragment that starts at residue 51, continues through the linker joining the old N- and C-termini, and finally ends at residue 46. The result is a gene that codes for permuted streptavidin, but lacks the four residues that make up the loop and places its new termini at the resulting gap. To indicate where the new termini are located, the mutant is labeled CP51/46. In this style of nomenclature, "CP" indicates a circular permutation and "51/46" indicates that the new N-terminus is where the original residue 51 was, and that the new C-terminus corresponds to residue 46 of the wild-type structure.

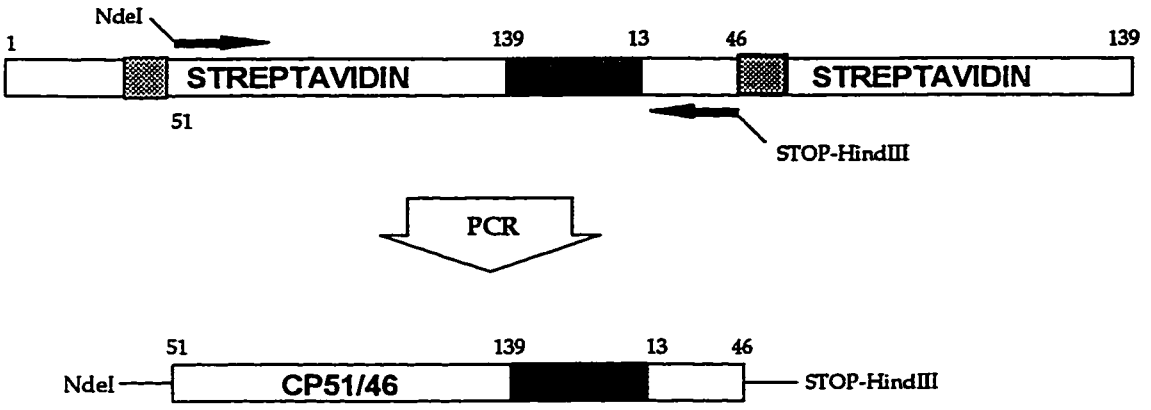

Figure 4. CP51/46 gene construction from tandem gene

PROTEIN SYNTHESIS AND PURIFICATION

CP51/46 was expressed under the control of the T7 promoter and purified as described in Chapter 2 of this document. No unusual measures were necessary to obtain adequate amounts of concentrated, purified CP51/46.

ISOTHERMAL TITRATION CALORIMETRY

To determine the $\Delta H°$ for the binding of biotin to CP51/46, samples were titrated with biotin on a CSC4200 Calorimeter (Calorimetry Sciences Corporation. Provo, UT) at 25°C. A 1.00mL solution of 10.7μM (subunit concentration) CP51/46 was titrated with 20 x 6μL injections of 250μM biotin. After adjusting for the heat of mixing as determined from the peaks measured after full titration, the $\Delta H°$ was determined by non-linear, least-squares fitting of the titration curve using the Bindworks software package. Since the K_a value fell in the range 10^5–10^9, a reliable estimate of the binding constant was also extracted from the isotherms via the same fitting function.

X-RAY CRYSTALLOGRAPHY

Creation of the protein crystals, collection of diffraction data, and refinement of the protein structure were performed by S. Freitag and I. Le Trong as part of our collaboration with the Biomolecular Structure Center. The details of the methods used are described in a separate publication.[15]

SURFACE AREA ANALYSIS

The ASAcalc program was used to calculate accessible surface areas for bound and unbound CP51/46.[76] The results are discussed in Chapter 5 of this document.

RESULTS

PROTEIN SEQUENCE

The CP51/46 mutant has an unprocessed N-terminal methionine as demonstrated by high resolution electrospray mass spectrometry and N-terminal sequencing. The potential contributions of this residue must be considered. It is, however, disordered and not observed in the crystallographic structures for either the biotin-bound or unbound states.

THERMODYNAMICS OF BIOTIN BINDING TO CP51/46

Isothermal titration calorimetry was used to characterize the thermodynamic consequences of deleting residues 47 through 50 of the flexible loop (Figure 5).

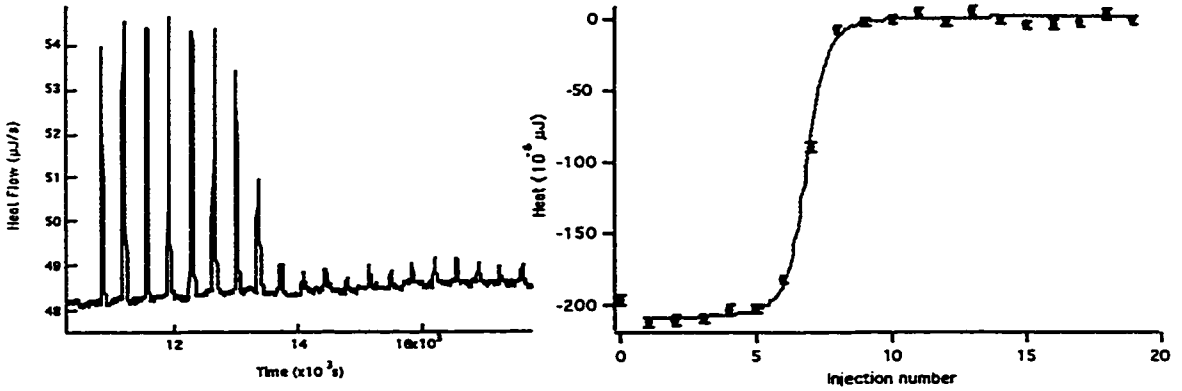

Figure 5. Sample ITC isotherm (left) and independent binding site fit (right) of CP51/46 at 25°C used to determine K_a and $\Delta H°$

From the K_a, $\Delta G°$ can be calculated according to the equation: $\Delta G° = -RT\ln K_a$. Knowing $\Delta G°$ and $\Delta H°$ allows the calculation of $T\Delta S°$ from $\Delta G° = \Delta H° - T\Delta S°$ (Table 2).

Table 2. Equlibrium parameters for CP51/46 at 25°C

	Wild-Type	CP51/46
K_a (M^{-1})[a]	$2.5 \cdot 10^{13}$	$(2.3 \pm 0.4) \cdot 10^{7}$
$\Delta G°$ (kcal/mol)	-18.3	-10.0±0.1
$\Delta H°$(kcal/mol)	-24.9±0.4	-13.8±0.8
$T\Delta S°$ (kcal/mol)	-6.6±0.4	-3.8±0.7
ΔC_p (cal/mol·K)[b]	-345±12	-95±29

[a] K_a value for WT from Green, 1990
[b] ΔC_p value for WT from Freitag, 1998

WT streptavidin displays a K_a that has been estimated to be 2.5×10^{13} M^{-1}, and we have previously determined the standard binding enthalpy to be -24.9 kcal/mol at 25°C.[2,

10] Using the estimated K_a and associated standard Gibb's free energy, the $T\Delta S°$ term for wild-type streptavidin would then be -6.6 kcal/mol at 25°C. With the CP51/46 mutant, the K_a for biotin is reduced approximately six orders of magnitude to 2.28 x 10^7 M^{-1} ($\Delta G°$ = -10.0 kcal/mol) at 25°C. The association of biotin is still enthalpically driven with a $\Delta H°$ of -13.8 kcal/mol and the $T\Delta S°$term is -3.8 kcal/mol at 25°C. The enthalpy values in both phosphate and Tris buffers are within experimental error of each other, suggesting that protonation effects are not significant in the mutant despite the introduction of charged termini at the binding site.

The change in heat capacity was also measured for CP51/46 to provide further thermodynamic insight into the role of the loop. The ΔC_p was significantly less negative at -95 ± 29 cal/mol·K compared to the value of at -345 cal/mol·K for wild-type streptavidin. This alteration is qualitatively consistent with the expected decrease in surface area buried in the CP51/46 bound state after loop deletion. Previous analysis of the avidin-biotin system by Spolar and Record suggested that ΔC_p for biotin association is dominated by the folding of the loop residues.[52]

X-RAY STRUCTURES OF CP51/46

The crystal structure of unbound CP51/46 was determined at 2.0 Å resolution. Comparisons of the overall fold of the CP51/46 tetramer with other core-streptavidin structures indicate no major differences: Least squares fits of the β-sheet C_α atoms of CP51/46 tetramer onto the monoclinic wild-type structures (PDB files: 1SWA, 1SWB, 1SWC) result in rms distances (RMSDs) between the C_α atoms of 0.3 Å in all cases. Fits performed by mapping only one subunit at a time (rather than the entire tetramer) give RMSDs of 0.2 Å for the fitted subunit and values in the range of 0.2 to 1.0 Å for the other three. Superpositions of the four individual CP51/46 subunits onto each other show no significant differences (RMSDs=0.2 Å).

The crystal structure of the biotin-bound complex of CP51/46 was also determined and was refined at 1.8 Å resolution. Electron density for biotin was clearly defined for all atoms in biotin. The results here also suggest a very high degree of similarity with the original wild-type structure: The RMSD after superposing 4 x 65 C_α atoms of the CP51/46-biotin complex on the wild-type-biotin complex structure is 0.3 Å. Rotation of the wild-type tetrameric complex onto that of CP51/46 based on superposition of only one subunit, gives RMSDs of 0.2 to 0.3 Å for the fitted subunit and 0.3 to 0.7 Å for the other three subunits.

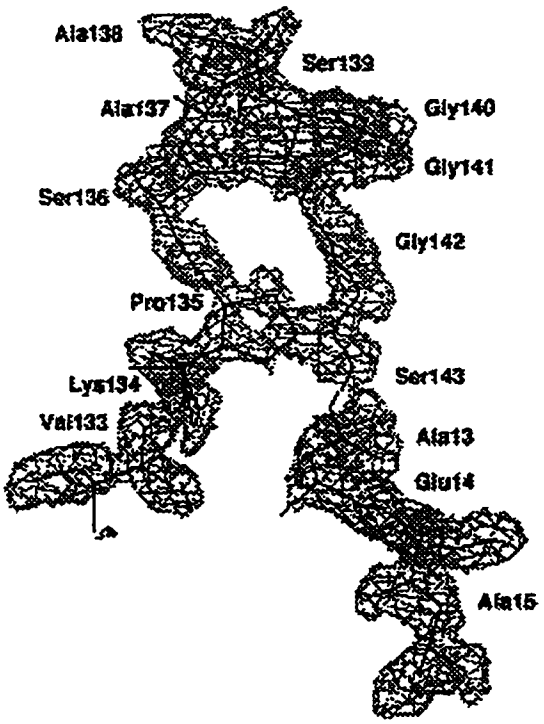

Figure 6. Linked termini in CP51/46

While the overall structure of CP51/46 is the same as that of wild-type streptavidin, there are structural changes at the two regions where the protein was specifically altered. The first is located at the site of the original termini: All of the residues comprising the original chain ends and the new linking sequence between them are ordered and clearly visible in two of the four subunits of the unbound CP51/46 tetramer. Residues 13 to 15 and 134 to 139 have been disordered in other monoclinic wild-type structures[14], but here they can clearly be identified along with the four new residues—Gly140, Gly141, Gly142, and Ser143. The ordering of two of the four connecting loops appears to be due to packing interactions in the crystal form; presumably, all of the loops would remain disordered and flexible in solution. The linking loops are not visible in any of the subunits of the bound CP51/46 structure. As this is clear evidence of the union of the original chain termini, we are confident that the protein was successfully permuted.

Figure 7. CP51/46 Tetramer [15]

The second structural change occurs at the binding site where we had planned to excise the flexible loop. Three residues at the new N- and C-termini are disordered in the unbound structure and unobserved in electron density maps. The N-terminal methionine is not seen in the electron density of either the unbound or bound forms (despite the presence of a relatively heavy sulfur atom in the side-chain) indicating that the residue is highly mobile. Residues Glu51 and the C-terminal residue Ala46 are also mobile and invisible in electron density maps. The first observed terminal residues are

Ser52 and Ser45, which show distinctly higher B-values for main- and side-chain atoms than are found in the rest of the structure.

A comparison of unbound CP51/46 in this region with unbound wild-type structures reveals a great deal of similarity. One of the key differences between the unbound and complexed structures of wild-type streptavidin is the breakage of a hydrogen bond in the β-sheet structure which flanks the loop upon biotin binding.[14] The last β-sheet hydrogen bond in the wild-type unbound state between strands 3 and 4 is the one from the nitrogen of Ser45 to the carbonyl oxygen of Ser52. This interaction is also observed in unbound CP51/46. In wild-type-biotin complexes, this hydrogen bond breaks and is accompanied by the formation of a hydrogen bond between Ser45 Oγ and the ureido nitrogen atom of the bound biotin. In the complexed CP51/46 structures, this set of events also occurs.

In all four subunits in the CP51/46-biotin complex, electron density for biotin was detected in the same orientation as in the wild-type biotin complex. The only differences in the hydrogen bonding patterns are omissions arising from deletion of the loop residues. In the wild-type complex, one of biotin's carboxylate oxygen atoms is hydrogen bonded to the amide of Asn49, but the deletion of the binding loop removes this interaction. All other first shell hydrogen bonds are very similar to those found in the wild-type complex. The second shell of hydrogen bonds is disturbed by the deletion Val47 which normally interacts with Ser45 in the wild-type protein.

The flexible linker joining the "old" termini (13 and 139) exhibited order along its entire length and apparently forms a large number of hydrogen bonds with adjacent subunits in the crystal. The X-ray structure clearly shows that the previous set of termini are now part of the protein backbone which strongly suggests that the new termini have, in fact, been moved to the positions of residues 51 and 46. There was some worry that since full-length streptavidin (with its complete N- and C-terminal

sequence) has a tendency to aggregate, that putting a linker between the old termini might re-create that tendency.[77] Given the solubility and refolding characteristics of the CP51/46 mutant, this does not appear to be the case.

DISCUSSION

Flexible loops near active sites or binding sites have been seen to provide a variety of enhancements to the association of protein and ligand. In many cases, they act as gates that open to optimize substrate/ligand association and close upon binding to prevent solvent access and to form bonding contacts that minimize dissociation. Much of the work with flexible loops has been conducted in the context of enzymatic catalysis, where site-directed mutagenesis and crystallographic studies have probed their contributions to various states in the turnover cycle. The detailed thermodynamic contributions of flexible loops to small molecule recognition, however, have not been well studied. Few analyses discuss the loops' roles in terms of the free energy breakdown into enthalpic and entropic components. One theoretical consideration of flexible loop closure in the avidin-biotin system predicted that the energetic signature of biotin binding should resemble that of protein folding since the process involves the partitioning of several loop residues from a solvent exposed state to a bonded, non-exposed state.[52] We have used a circular permutation approach to delete the streptavidin flexible binding loop in a manner not previously reported in the literature and studied both the structural and the thermodynamic consequences.

In the case of CP51/46, the circular permutation approach leaves free ends at the base of the flexible loop rather than the peptide connection left with standard deletion techniques. Comparison of the wild-type and circularly permuted streptavidin structures demonstrates that there are no significant quaternary changes introduced by the loop deletion. Similarly, the introduction of the residues joining the native N- and C-termini does not affect the structure of the tetramer. As this engineered connector is

observed only in subunits where the loop is involved in crystal packing interactions, it is assumed that the connector is disordered in solution.

A detailed analysis of the CP51/46 biotin-binding residues demonstrate that the conformations of all of the direct hydrogen bonding and aromatic contacts are indistinguishable from wild-type in both the unbound and complexed states. A remarkable feature of the CP51/46 structural analysis is the retention of coupled hydrogen bonding alterations in the loop hinge points upon biotin association that are seen in wild-type. A previous crystallographic analysis of the flexible loop showed that the open conformation is stabilized by a β-sheet hydrogen bonding interaction between Ser-45 of the β-strand leading into the loop and Ser-52 of the β-strand leading out of the loop. This hydrogen bond is broken in the closed conformation as the side-chain hydroxyl of Ser-45 moves into position to hydrogen bond to a ureido nitrogen of biotin. That this structural alteration between Ser-45 and Ser-52 is preserved in the loopless CP51/46 mutant implies that the formation of the Ser-45 side-chain hydrogen bond to biotin may drive the conformational closure of the loop rather than *vice versa*. The overall conservation of structure between wild-type and CP51/46 suggests that any thermodynamic changes that are observed should attributable primarily to effects arising from the deletion of the four loop residues in CP51/46.

Even though almost all of the direct binding contacts to biotin are retained, the CP51/46 mutant displays a dramatic decrease in affinity of approximately six orders of magnitude when compared to wild-type. This reduction in binding free energy is driven by a large decrease in the binding enthalpy ($\Delta H°$) which is lowered from -24.9 kcal/mol to -13.8 kcal/mol at 25° C. Qualitatively, it could be hypothesized that loop removal would result in a decrease in binding enthalpy since the N49 hydrogen bond to the biotin carboxylate is deleted along with any potential van der Waals interactions of residues 47 through 50. Nevertheless, the loss of four residues—only one of which appears to make direct contact with biotin—would not be expected to create such a

large (11.1 kcal/mol) change in the binding enthalpy. Examination of the CP51/46-biotin complex crystal structure reveals what a purely thermodynamic analysis would not have predicted: Residues 46 and 51 are also disordered in the bound state as a result of the loop deletion. Perhaps part of the large enthalpy change may be explained if the net effect of the mutations more closely resembles the removal of *six* residues (46–51) rather than four. The mobility of Ala-46 and Glu-51 may effectively create a much larger "window" over biotin when it is in the binding pocket.

With the removal of most of the loop, one might also predict that the binding entropy change would become less negative due to the reduction in configurational entropy penalties associated immobilizing all of the loop residues upon closure. The magnitude of this entropic effect might be tempered somewhat if the newly introduced chain termini were immobilized on biotin binding, but this does not appear to be the case. If a K_a of 10^{13} is assumed, then the $T\Delta S$ term is less negative by about 3 kcal/mol at 25° C indicating that the entropic costs of binding the ligand have been reduced. However, this value is strongly dependent on the widely-accepted value for K_a of 2.5 x 10^{13} determined by Green[2]—a value that has not been independently confirmed in the literature or in our lab due to the difficulties of obtaining accurate values for high-affinity binding constants. A K_a which was higher by a factor of 100 (10^{15}) would leave an unaltered $T\Delta S°$ term and allow interpretation of loop deletion effects in terms of the enthalpic consequences only.

CONCLUSION

We have used the technique of circular permutation to investigate the thermodynamic contribution of a flexible loop to the high-affinity streptavidin-biotin complex. The binding loop was removed while retaining the original conformation of the streptavidin tetramer as demonstrated by X-ray diffraction. The result was a drastic reduction in binding affinity which appeared to be driven mostly by a reduction in the magnitude of

the binding enthalpy. While this mutant demonstrates the importance of the binding loop to the creation of a high-affinity interaction between streptavidin and biotin, further experiments need to be performed to clearly define how the loop accomplishes its role in keeping biotin tightly bound.

CHAPTER 4: BINDING SITE LOOP DISCONTINUITY

INTRODUCTION

To further probe the role of the flexible loop, two mutants—CP50/49 and CP49/48—were created to generate discontinuities in the loop on either side of Asparagine-49 (N49). Residue 49 is hydrogen-bonded to a carboxylate oxygen of biotin in the bound complex via the main chain nitrogen. By cutting the loop at position 49, we are testing the hypothesis that the hydrogen bond of N49 is in some way responsible for maintaining the closed position. If this is true, then whichever half of the loop contains residue 49 should be able to achieve the closed position when biotin binds, and the other half should remain disordered. If, on the other hand, it is the breaking of the Serine-45 to Serine-52 hydrogen bond that nucleates loop closure, then we may see full or partial ordering of the loop halves regardless of which half contains residue 49. Since the wild-type N49 hydrogen bond is from a main chain atom rather than a side chain atom, a third possibility is that we might see a different loop residue form a main-chain hydrogen bond to biotin as the pieces of the loop achieve a new equilibrium position in the bound state.

In the literature on flexible loops, there is only one study of loop function investigated by nicking of the loop. The binding site loop of dihydrofolate reductase was nicked using a protease: The separate ends of the nicked, binding-site loop appear to close independently so that, even though the catalytic ability of the enzyme is compromised, the reaction intermediate is still protected from decomposition by water.[49] Similar behavior is possible in the streptavidin-biotin system if van der Waals interactions on both halves of the loop are responsible for creating the closed conformation.

MATERIALS AND METHODS

GENE CONSTRUCTION AND PROTEIN EXPRESSION

The genes for CP50/49 and CP49/48 were designed and constructed with the help of Saurabh Gupta and Cyndi Long. Both genes were created from the tandem streptavidin gene described in Chapter 3 using PCR mutagenesis.

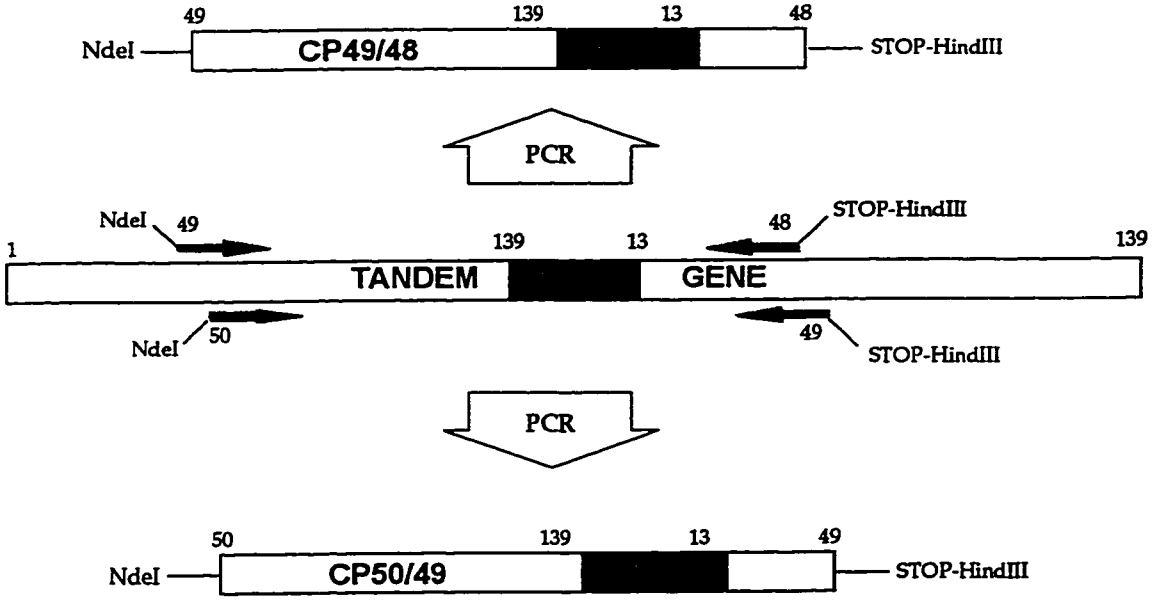

Figure 8. Construction of "Nicked Loop" CP streptavidin mutants

Protein synthesis was carried out using the T7 promoter system in BL21(DE3) cells (Novagen. Madison, WI) as previously described in Chapter 2. Both proteins expressed and refolded in a manner similar to that of wild type. Both mutants also retained sufficient binding affinity to allow purification over an iminobiotin column (Pierce. Rockford, IL).

Protein Characterization

Mass spectrometry and radiometric assays for kinetic and equilibrium thermodynamic parameters were performed as described in Chapter 2. Isothermal titration calorimetry experiments were performed as before with one change: The sample cell is completely filled with protein solution before the addition of titrant. This removes the air space above the sample and produces isotherms with much better signal-to-noise ratios. The data analysis procedure was altered to correctly reflect the new, constant-volume experimental conditions.

RESULTS

Electrospray mass spectrometry results indicate that while the CP50/49 mutant expressed correctly, the CP49/48 mutant still retains its initiating methionine. The expected molecular weight of both CP mutants was 13529. For CP50/49 the experimental value was 13530 and for CP49/48, 13656. The difference between expected and observed molecular weights in CP49/48 is exactly accounted for by the addition of a methionine residue at the N-terminus. Therefore, CP49/48 has a binding site loop which is not only discontinuous, but which also contains an extra residue just ahead of position 49. Interpretation of the effects of nicking the loop in CP49/48 would be confounded by possible effects from the addition of the methionine. The effect of a net addition to the binding site loop cannot be fully appreciated until a biotin-bound structure of CP49/48 is determined and the involvement (if any) of the extra methionine in the binding process ascertained. SDS-PAGE analysis of the purified proteins indicated electrophoretic mobility for both mutant tetramers and monomers virtually identical to those of wild-type streptavidin.

In both CP50/49 and CP49/48, the enthalpy of binding ($\Delta H°$) has been reduced in magnitude by 7.5–8.0 kcal/mol at 37°C. Additional experiments on CP50/49 reveal that the binding affinity (K_a) has decreased by a factor of 417 from the wild-type value

which translates into a 3.7 kcal/mol reduction in the magnitude of the free energy of binding ($\Delta G°$). From the free energy relationship, $\Delta G° = \Delta H° - T\Delta S°$, we have determined that these changes are accompanied by a 3.8 kcal/mol reduction in the entropic penalty associated with forming the complex.

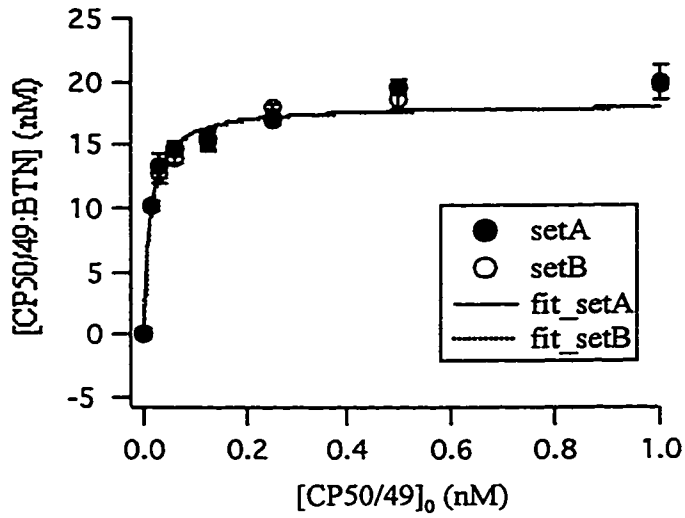

Figure 9. Competition curve of CP50/49 vs. 50 nM WT

ITC experiments over the temperature range 10°C–37°C reveal that the changes in heat capacity for CP50/49 (-145 cal/mol·K) and CP49/48 (-166 cal/mol·K) are not as steep as the wild-type value (-345 cal/mol·K). Differential scanning calorimetry of CP50/49 further reveals a surprising result: The melting point of CP50/49 (87°C) is *higher* than that of WT (79°C).

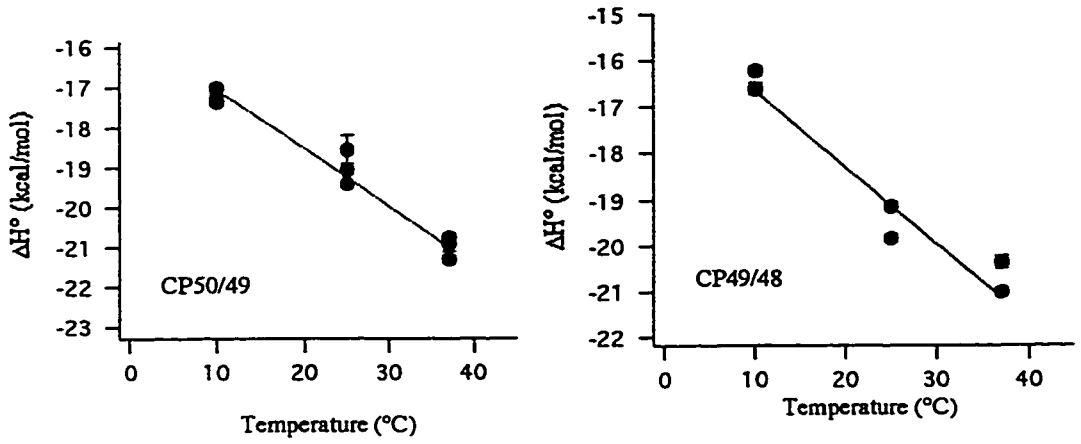

Figure 10. ΔC_p fits for CP50/49 and CP49/48

Transition state analysis of CP50/49 and CP49/48 uncovers more alterations to the binding reaction. In both mutants, the dissociation rate (k_{off}) of biotin has increased. The off-rate for CP49/48 is faster than that of CP50/49 at all temperatures and approaches the resolution limit of our radiometric assay at 25°C (Figure 10. The poor fit of the 298K point is likely to be an artifact of the assay as sampling times approach the half-life of biotin dissociation). For CP50/49, the k_{off}, when extrapolated to 37°C, is predicted to be 811 times faster than WT; for CP49/48, approximately 10000 times faster. The lowering of the dissociation barriers is, in contrast to the decrease in affinity, entropically driven rather than enthalpically driven. Both mutants exhibit an increase in gained entropy during biotin dissociation as compared to WT. For CP50/49, the difference is 3.2 kcal/mol, and for CP49/48, preliminary experiments estimate the additional entropic gain to be about 14.7 kcal/mol. CP50/49 retains the WT value for the enthalpic barrier to dissociation; CP49/48 has a compensating increase in $\Delta H^{\ddagger}$ which may be the result of interactions with the extra methionine on the biotin exit pathway.

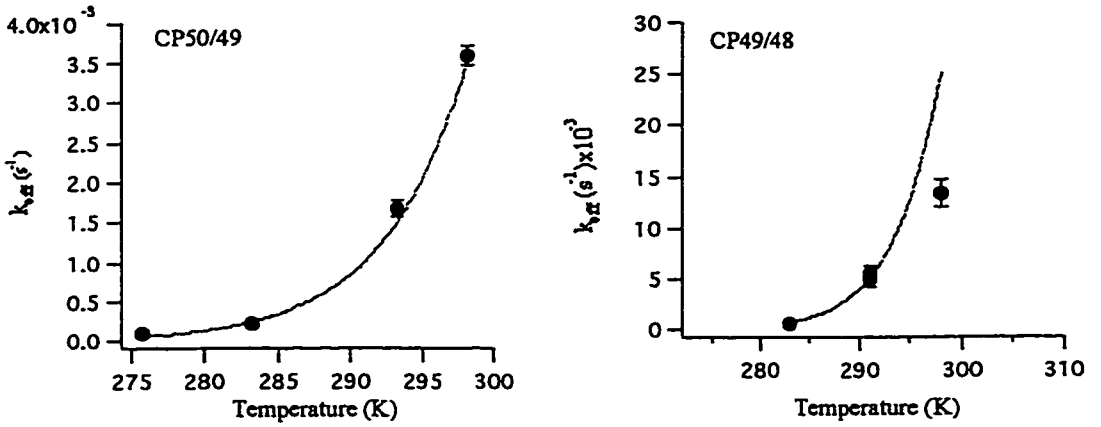

Figure 11. Eyring equation fits for CP50/49 and CP49/48 from k_{off} data obtained at different temperatures.

DISCUSSION

The role of flexible loops near binding sites has previously been studied in the context of enzymatic reactions where they have been seen to enhance catalysis either by bringing reactive side chains into proximity or by retaining and protecting reaction intermediates. In the streptavidin-biotin system, the binding site loop also achieves an ordered, closed conformation upon biotin binding. In this case, there is no reaction and no unstable intermediate to protect so the role of the loop is less clear. We may postulate two possible roles for the loop:

1. Enhancement of binding enthalpy through additional hydrogen-bonds and van der Waals contacts.
2. Increasing the barrier to dissociation through steric retention of biotin.

If these hypotheses hold true, then the thermodynamic signature expected from removal of the loop would be reduction of binding enthalpy and an increase of dissociation rate. In the CP51/46 mutant where most of the loop is removed, this is exactly the signature which is observed.[15]

There remain, however, additional questions regarding the loop which could not be answered by deletion. For example, the enthalpic/entropic balance of the dissociation barrier could not be determined in CP51/46. Also, while the entropic penalty for binding was reduced by 2.4 kcal/mol, can that difference be assigned on a per residue basis to the segment which no longer needs to be ordered? To answer these questions, we created two more circular permutations of streptavidin in which the loop was cut on either side of a putative anchor point—N49.

CP49/48

Unfortunately, the initiating methionine remains on CP49/48 which complicates the analysis. The few experiments on CP49/48 imply equilibrium parameters very similar to those of CP50/49 including nearly identical values of $\Delta H°$. Although a relative K_a has not been determined for CP49/48, the shape of its ITC isotherms suggests a K_a very close to that of CP50/49 as well. The preliminary transition state analysis of CP49/48 indicates that it has markedly different kinetic behavior though. The values of $\Delta H^{\ddagger}$ and $\Delta S\ddagger$ appear to be much larger than those of either WT or CP50/49 implying a significant change in the dissociation pathway. This may be due to hydrophobic or steric contacts with the extra methionine on the exit pathway. To remove the confounding effect of the methionine, it would be more appropriate to study a CP49/48 variant with a mutation at position 49 to promote removal of the initiating methionine—to alanine, glycine, proline, or serine, for example.[78] Since the N49 hydrogen bond to biotin is from the main chain nitrogen rather than the side-chain, the potential for re-forming the position 49 hydrogen bond to biotin remains even though other effects may arise from the mutation to an amino acid other than asparagine.

Table 3. Thermodynamic comparison of WT, CP50/49 and CP49/48 at 37°C

Parameter	WT	CP50/49	CP49/48
K_a ratio (MUTANT:WT)	—	417±14	—
$\Delta\Delta G°$ (kcal/mol)	—	+3.7±0.1	—
$\Delta\Delta H°$ (kcal/mol)	—	+7.6±0.1	+7.9±0.1
$T\Delta\Delta S°$ (kcal/mol)	—	+3.8±0.1	—
ΔC_p (cal/mol·K)	-345±12	-145±3	-166±3
$T_{melting}$ (°C)	79	87	—
k_{off} (s^{-1})	$2.9 \cdot 10^{-5}$	0.024	0.33
$\Delta G^{\ddagger}$ (kcal/mol)	24.6	20.5±0.9	18.8±1.3
$\Delta H^{\ddagger}$ (kcal/mol)	30.4	29.5±0.4	39.3±0.6
$T\Delta S^{\ddagger}$ (kcal/mol)	5.8	9.0±0.5	20.5±0.7

CP50/49

Complete thermodynamic and kinetic characterization of the CP50/49 mutant reveals that a nicked binding site loop still retains partial function when compared with the deleted loop of CP51/46. The nature of this function is manifested in a reduction of the magnitude of enthalpy for the binding reaction with no change in the enthalpic component of the dissociation barrier. This implies that the loop is already open and does not contact biotin in the transition from bound to unbound states, but that it does contribute to the stability of the bound complex. The entropic penalty for binding biotin is lower than that of WT by 3.8 kcal/mol. Had both loop segments become ordered on binding, we would expect the entropic penalty to increase as a result of the additional degrees of freedom lost in the immobilization of the chain termini versus immobilization of the intact loop. This value of $T\Delta\Delta S°$ is still less than that for deletion of the full loop in CP51/46 suggesting that partial ordering of one or both of the loop segments occurs.

Despite the lowered entropic penalty for binding, the overall binding affinity drops by approximately 400-fold compared to WT as a result of changes in the enthalpy of

binding. The reduction in the magnitude of ΔH° and the drop in binding affinity are both less drastic than the changes seen in CP51/46 as was expected in a mutant designed to retain some functionality in the loop.[15] The enthalpic destabilization of the bound complex could be interpreted in terms of loss of enthalpic contacts with the loop including the hydrogen bond from N49 and van der Waals interactions between the distal portion of the valeryl tail and loop residues.

The kinetics of biotin dissociation from CP50/49 display a different sort of change. The salient points are a dissociation rate that is about 800 times faster than that of WT, an enthalpic dissociation barrier ($\Delta H^{\ddagger}$) which is unchanged, and a 3.1 kcal/mol increase in the entropy gained ($T\Delta S^{\ddagger}$) when biotin exits. The similarity of $\Delta H^{\ddagger}$ to the value in WT suggests that the same number and type of enthalpic contacts must be broken for dissociation to occur even though the loop has been altered. From this, one might conjecture that the loop has few bonding contacts and that its role is primarily to increase the residence time of biotin in the binding site by sterically hindering its escape. The increase in entropy gain on dissociation is consistent with the signature expected from the increase in configurational entropy from mobilization of chain termini instead of a continuous flexible segment.

An additional complicating factor in the interpretation fo the thermodynamic and kinetic data common to all CP mutants is the introduction of charged residues wherever the original chain is cleaved to form new termini. In the case of CP50/49 and CP49/48, the new termini are residues that, while not constrained to remain adjacent, are likely to remain in close proximity. The potential formation of a salt bridge between the termini would serve to ameliorate the consequences of removing the original peptide bond. Another possibility is that the chain ends could interact with the negatively-charged carboxylate of biotin thereby creating an additional bonding interaction where one was not present before. The results from structural analysis of CP51/46 suggest that this is unlikely. In CP51/46, the initiating methionine is retained so that the positively-

charged N-terminus is essentially at position 50; this is exactly the location of the N-terminus in CP50/49. No interaction of the N-terminus with biotin is observed in CP51/46, but definitive statements on the role of the N-terminus in CP50/49 will have to await determination of the structure.

CONCLUSION

In creating a nicked-loop variant of streptavidin using circular permutation, we have further highlighted the importance of the flexible loop in creating the high-affinity interaction of streptavidin and biotin. Here, we have not mutated or removed any binding-site residues; merely broken the protein chain in a highly-mobile surface loop. The result is a drop in affinity and a large increase in biotin dissociation.

With the current thermodynamic and kinetic data, we propose that some portions of the loop are able to attain a "closed" configuration over the binding site, but that both halves do not close independently to recreate the fully closed position. Were that the case, we would expect to see an increase in the entropic penalty for binding. But the reverse is true. The loop plays a role in enthalpic stabilization of the bound state, and the entropic penalties of immobilizing a flexible portion of the protein to enhance binding are kept to a manageable level by using a contiguous loop of medium length (6 residues) which is already constrained by its anchorage to strands of the β-sheet. More definitive interpretations of the effects of this mutation must await the solution of the structure for the CP50/49-biotin complex.

CHAPTER 5: STRUCTURAL THERMODYNAMICS

INTRODUCTION

STRUCTURAL THERMODYNAMICS

In its most ideal form, structural thermodynamics is the prediction of the stability or binding affinity of a protein or protein-ligand system purely from its three-dimensional structure. In many respects, it is the natural extension of the protein folding problem wherein researchers attempt to predict the three-dimensional structure of a protein solely from its amino acid sequence. Recent studies have indicated that the structural thermodynamics problem is perhaps a bit more tractable than that of protein folding. If protein thermodynamics could be reliably predicted from structural data, the fields of protein engineering and rational drug design would receive a tremendous boost. The effects of site-directed mutations on ligand-binding could be predicted beforehand which would allow directed optimization of binding affinities.[79]

ACCESSIBLE SURFACE AREA

Functionally, the predictive information which needs to be extracted from the three-dimensional structure is the accessible surface area (ASA). "Accessible" means exposed to solvent, and the idealized "water molecule" which is used as a probe for accessibility takes the form of a sphere with 1.4 Å radius. There are a variety of methods for determining ASA, but the most popular are those devised by Connolly[80] and by Lee and Richards.[81] Connolly's surface is the accessible van der Waals surface of the protein atoms and the re-entrant surfaces that represent the maximum penetration of the probe sphere into the interstices as determined by the *surface* of the probe; it is essentially a *contact* surface. By contrast, the Lee and Richards accessible surface is the locus of points traced by the *center* of the probe sphere; it is the

intersection of surfaces if all the protein van der Waals radii were to be expanded by 1.4 Å. There exist other methods for calculating surface area[82-85], but the most of those are refinements of the original Lee and Richards algorithm.

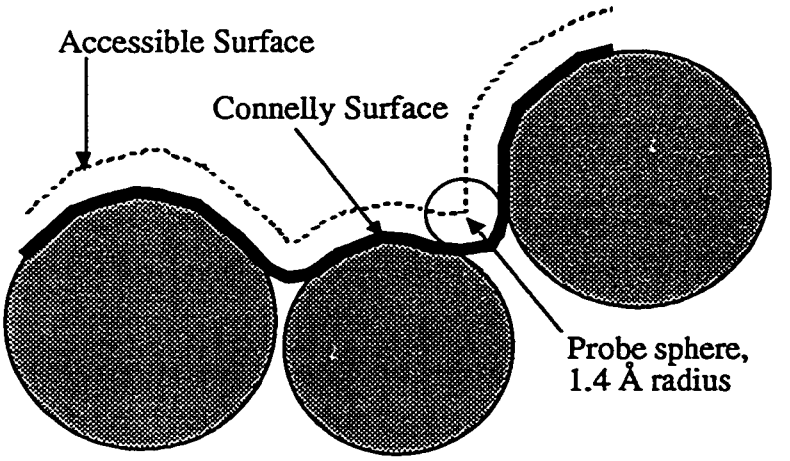

Figure 12. Accessible surface vs. Connelly surface

MODEL COMPOUND STUDIES

The bases for predicting protein behavior from structure may be found in studies where hydrocarbons[86] and other model compounds were transferred into aqueous solution. It was discovered that a high correlation existed between the thermodynamic properties of the transfer and the exposed surface areas of the compounds. From there, the concept was expanded to proteins when it appeared that the larger macromolecules also exhibited the same correlation for folding from the denatured state.

Livingstone, *et al.* observed that protein folding involved the removal of nonpolar surface area from water and that the ΔC_p's measured for that process appeared to have the same surface area dependence as that ΔC_p's for transfer of hydrocarbons from aqueous solution back to the pure liquid state.[87] Using a variation of the Lee and

Richards algorithm developed by Richmond[85], they demonstrate that the ΔC_p's of 14 proteins and 12 hydrocarbons exhibit similar linear dependencies on accessible, nonpolar surface area:

Hydrocarbons: $\Delta C_p = (-0.32 \pm 0.03)\, \Delta ASA_{npolar}$

Proteins: $\Delta C_p = (-0.25 \pm 0.03)\, \Delta ASA_{npolar}$

ΔC_p is expressed in cal/mol·K and ΔA_{np} in $Å^2$. The basis for the decrease in heat capacity with removal of nonpolar surface area (a negative ΔASA_{apolar}) is the hydrophobic effect. Loss of ordered-water clathrate structures around exposed hydrophobic areas, which are characterized by high heat capacities and low entropies, reduces the heat capacity of the system.[88] Murphy and Gill would later perform experiments involving transfer of cyclic dipeptides into water and refute the premise that ΔC_p could be explained only by changes in nonpolar surface area. They demonstrated that the polar surface area made a large, and opposing, contribution to ΔC_p. They also proposed an explanation for the linear correlation of $\Delta H°$, $\Delta S°$, and ΔC_p based on the additive effects of four groups: peptide bonds, apolar hydrogens, aromatic rings, and hydroxyls.[89] Livingstone, Spolar, and Record responded with a publication of transfer data for organic amides and modified their model to include polar contributions to the folding process:

RELATIONSHIP OF ΔC_p TO ACCESSIBLE SURFACE AREA

Freire's group has proposed a universal function for predicting the heat capacity of proteins from structural information.[90] They describe protein heat capacity (C_p) as the sum of four components:

1. Contributions from the covalent bonds of the primary structure.This accounts for the majority of a protein's heat capacity and may be parameterized in terms of a protein's size (MW).

2. Contributions from intramolecular non-covalent interactions. These are interactions resulting from the secondary or tertiary structure of the protein and scale with the amount of buried (vs. accessible) surface area.
3. Contributions from solvent interactions. In this case, "solvent" means water and the heat capacity effects arise from the differing interactions of nonpolar and polar areas on the surface of the protein with surrounding water—$ASA_{nonpolar}$ and ASA_{polar}, respectively.
4. Contributions from protonation events. These contributions are usually on the order of a few calories/mol·K, but may become significant if the pH of a non-buffered solution containing the protein is at the pK_a of ionizable side-chains (e.g. histidines) of the protein.

In the specific case of ligand binding, we are interested in changes in the heat capacity (ΔC_p) between the bound and unbound states. Since contributions 1 is not expected to change as a result of binding, ΔC_p must arise from contributions 2 and 3 (and perhaps 4 if a protonation event occurs on binding also). Therefore, to a first approximation, the prediction of ΔC_p from structural data relies upon deriving an accurate relationship between ΔC_p and the *changes* in accessible surface area, ΔASA_{apolar} and ΔASA_{polar}.

PARAMETERIZATIONS

The goal of these investigations into the relationship between heat capacity and surface area is ultimately the calculation of all the equilibrium parameters for the folding of a protein for which the structure has been determined. After calculating the ΔC_p from ΔASAs, $\Delta H°$ and $\Delta S°$ could be calculated as follows:

$$\Delta H°(T) = \Delta H°(T_H^*) + \Delta C_p(T - T_H^*)$$

$$\Delta S°(T) = \Delta S°(T_S^*) + \Delta C_p \ln(T/T_S^*)$$

In this case, T_H^* and T_S^* are reference temperatures at which $\Delta H°$ and $\Delta S°$ converge to common values for all proteins. The value of T_H^* is 100°C and that of T_S^* is 112°C.[79, 91] Naturally, $\Delta G° = \Delta H° - T\Delta S°$ would provide the remaining parameter.

These calculations hinge on whether or not we may obtain an accurate value for ΔC_p from structural data. Currently, there are two parameterizations for ΔC_p in the literature. Both are based on protein databases for which high-resolution structures and thermodynamic data are available. The values from Spolar, *et al* include data for the transfer of organic amides into solution and those Freire *et al* include data from solid dipeptide dissolution studies.

$$\textit{Spolar, et al:}\quad \Delta C_p = (-0.32 \pm 0.04)\,\Delta ASA_{npolar} + (0.14 \pm 0.04)\,\Delta ASA_{polar}$$

$$\textit{Freire, et al:}\quad \Delta C_p = (-0.45 \pm 0.02)\,\Delta ASA_{npolar} + (0.26 \pm 0.03)\,\Delta ASA_{polar}$$

More recently, studies have been performed which demonstrate that these calculations may also hold true for protein-protein and protein-ligand associations. Systems for which the calculated and experimental ΔC_p's agree well are Angiotensin II/Antibody[51], Grb2-SH2/Phosphotyrosine polypeptide[92], Lysozyme/HyHEL-5 Antibody[93], Endothiapepsin/Pepstatin A[94], FK506/FKBP-12[95], and Agglutinin/N-Acetylglucosamine[91].

MATERIALS AND METHODS

Isothermal titration calorimetry studies were carried out at temperatures from 10°C to 37°C. The change in heat capacity was determined from a linear, least-squares fit of $\Delta H°$ versus temperature.

Calculation of ASA was performed using ASAcalc[76] which is based on the Lee and Richards algorithm.[81] Calculations use a solvent radius of 1.4 Å and a slice width of 1.25 Å. The results are averaged over a set of 12 rotations (since slices are taken orthogonal to the z-axis, ASA is calculated using a number of axial orientations to eliminate artifacts arising from anisotropies in the calculation method.

To properly compare ASAs between WT and CP51/46, the structure files for each protein were modified in the following manner:

1. All water molecules and residues 13–15 and 133–139 were removed to reduce all sets to the common detected residues.
2. Copies of the open binding loop were added to subunits in which the open loop was disordered in unbound WT (pdb entry—1SWC).
3. ASA of free biotin was calculated by extracting the four biotins from the WT-biotin complex.

Apolar ASA was treated as the sum of ASAs from carbon and hydrogen atoms; Polar ASA from nitrogen and oxygen. Changes in ASA on binding (ΔASAs) were calculated as the difference of the complex ASA and the combined ASAs of the unbound protein and free biotin. For a given protein-ligand system, there exist three values of ASA of interest which may be calculated from structural data:

1. ASA of the protein alone in its unbound conformation
2. ASA of the ligand alone
3. ASA of the bound protein-ligand complex (which may be further divided into contributions arising from the protein or from the ligand alone)

The difference between 3 and 1+2 is what is normally thought of as ΔASA for a binding reaction. Since thermodynamic parameters for WT streptavidin and its mutants are expressed per subunit, the ΔASA values and calculated ΔC_p's are expressed as the average value per subunit also.

RESULTS

PREDICTED VS. OBSERVED HEAT CAPACITY

The surface area calculations for WT and CP51/46 reveal that biotin binding tends to bury a higher percentage of nonpolar surface area than polar. The proportions or more

evenly distributed in CP51/46 binding but still weighted toward a greater ΔASA_{apolar}. Using either scheme for parameterization, the calculated values of ΔC_p underestimate the actual value for WT and overestimate the value for CP51/46 (Table 4).

Table 4. Predicted ΔCp for WT and CP51/46

	WT	CP51/46
ΔASA_{apolar} (Å^2)	-566	-446
ΔASA_{polar} (Å^2)	-145	-234
Freire ΔC_p (cal/mol·K)	-217	-140
Livingstone ΔC_p (cal/mol·K)	-161	-110
Observed	**-345**	**-95**

It might be anticipated that deletion of the loop that closes over the biotin site would result in significantly larger solvent accessible surfaces for the biotin ligands in CP51/46. In fact, the changes are not all that large. The average solvent accessible surface for biotin in the wild-type complex is 18.3 Å^2, indicative of the nearly complete burial of biotin when bound to streptavidin. (The solvent accessible surface for "free" biotin is 407.2 Å^2). The only exposed biotin atoms are the carboxylate oxygen atoms. The accessible surface increases to 56.5 Å^2 for the CP51/46 complex. The oxygen atoms have become somewhat more exposed as have distal portions of the aliphatic chain. In terms of ΔC_p, this change in ASA for biotin would produce a mere 7 cal/mol·K change as a result of deleting the loop.

BREAKDOWN OF ACCESSIBLE SURFACE AREA CHANGES

To understand the disparity between predicted and experimental values for ΔC_p, the calculations for accessible surface area were dissected on a residue by residue basis (Figures 12 and 13). This analysis produced two results. First, it was possible to gain an overall picture of where surface area was being buried or exposed in WT and CP51/46 on binding. As expected, residues which make contact with biotin exhibit the

largest changes in ASA as a result of binding with a large number of changes occurring in loop 45–52 of WT. Overall, the ΔASA's are smaller in CP51/46 and, of course, no changes occur in the region of the excised loop.

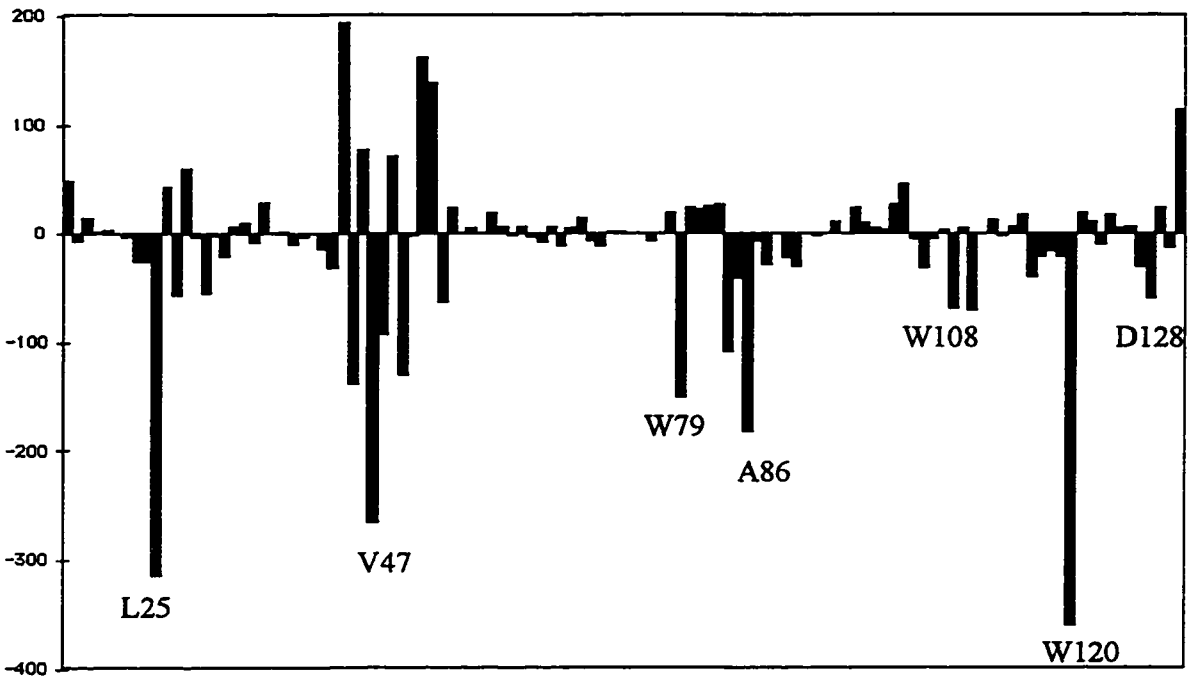

Figure 13. Accessible surface area changes in WT upon binding of biotin localized to specific residues. Y-axis scaled in Å^2.

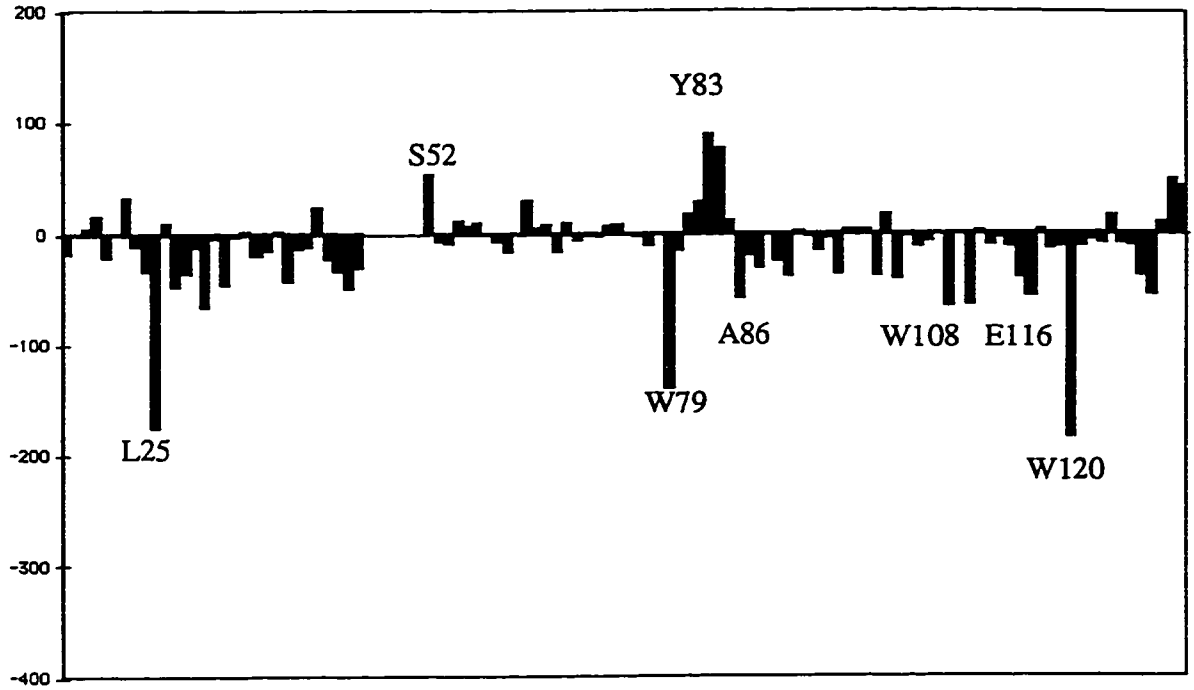

Figure 14. Accessible surface area changes in CP51/46 upon binding of biotin localized to specific residues. Y-axis scaled in Å^2.

Secondly, it was possible to limit the changes in ASA used for calculating ΔC_p to just those residues at the binding site (see Appendix B). The results of those calculations are shown in Table 5, and they reveal that the ΔASA changes resulting from loop deletion are mainly apolar in nature.

Table 5. Predicted ΔC_p for WT and CP51/46 calculated from binding site residues only

	WT	CP51/46
ΔASA_{apolar} (Å^2)	-515	-322
ΔASA_{polar} (Å^2)	-239	-230
Freire ΔC_p (cal/mol·K)	-170	-85
Livingstone ΔC_p (cal/mol·K)	-131	-70
Observed	**-345**	**-95**

From a comparison with the values for all the residues in the protein, it is apparent that a large number of residues away from the binding site contribute to the values for apolar and polar ASA, and that those contributions alter the balance of the respective categories of ASA.

DISCUSSION AND CONCLUSION

To test the applicability of current theories on structural thermodynamics to protein-small molecule interactions, we applied the analyses developed by the Freire and Livingstone laboratories to the WT and CP51/46 mutants and their complexes with biotin. We did not expect the individual ΔC_p values to match because the parameters relating them to changes in ASA are derived from a database of structural thermodynamic data for protein folding and significant deviations could arise from the specific properties of biotin, a small molecule. Nevertheless, the crystallographic analysis indicates that the similarities in biotin binding and the small differences in ASA should give rise to similar ΔC_p's. What is observed instead are calculated ΔC_p's that qualitatively predict the relationship for the values of WT and CP51/46, but which fail to quantitatively model the experimental values. This discrepancy between

predicted and calorimetrically-determined values has also been seen in the binding of antibodies to proteins such as lysozyme[96] and cytochrome *c*[97], in the binding of growth hormone to its receptor[98], and in the barnase-barstar interaction.[99]

Closer examination of the WT and CP51/46 structures reveals many side-chains away from the binding site that display significant alterations in ASA between the bound and unbound structures. As these residues do not participate in biotin binding, the total values of ΔASA appear to include changes that should not have an effect on the ΔC_p under the assumptions of this parameterization. This finding highlights the problem of using an isolated, static crystallographic structure to model the behavior of a protein in solution. Subtle changes in side-chain conformation across different subunits or even across different crystal forms of the same protein-ligand pair alter the total accessible surface area in ways which may have nothing to do with the binding event. Further investigation into methods for reconciling X-ray structures and bulk dynamic behavior of proteins under experimental conditions needs to be performed before this type of structural thermodynamic approach may be used to accurately predict binding behavior.

CHAPTER 6: ASPARTATE-128 AND BIOTIN EXIT PATHWAYS

INTRODUCTION

While the reaction coordinate model provides a useful context for understanding how enzymes manage activation barriers, there have been few attempts to model ligand binding reaction coordinates in the same manner. An important fundamental question is whether there even are defined ligand exit pathways that can be described by such a model. Do small molecules dissociate in a well ordered sequence of bond breaking and protein conformational events, or is it a stochastic process with many potential pathways and barrier topologies? In support of a defined pathway for biotin dissociation from streptavidin, we have observed a concerted shift of binding contacts while structurally characterizing an aspartate-to-alanine (D128A) mutant that closely mimics an intermediate on the dissociation pathway predicted by a potential of mean force (PMF) molecular dynamics simulation. Aspartate-128 is directly hydrogen bonded to a ureido nitrogen of biotin and also networks with the important aromatic binding contacts Trp-92 and Trp-108. The Asn 23 hydrogen bond to the ureido oxygen of biotin is broken in the D128A structure, and a water molecule has moved into the pocket to replace the missing Asp-128 carboxylate interaction. These alterations are accompanied by the coupled movement of biotin, the flexible binding loop containing Ser-45, and the loop containing the Ser-27 contact. Remarkably, these alterations are duplicated in a key intermediate observed in the PMF calculations. In the simulated pathway, the Asn-23 hydrogen bond breaks first. This is accompanied by the lengthening of the Asp-128 hydrogen bond to biotin and its subsequent replacement by an entering water molecule. Furthermore, both biotin and the flexible loop move in a concerted conformational change that mimics the D128A structural changes. Our composite results suggest that the D128A mutant provides a structural "snapshot" of an early intermediate on a well defined biotin dissociation pathway.[100]

MATERIALS AND METHODS

GENE CONSTRUCTION & PROTEIN EXPRESSION.

The gene for the D128A mutant was constructed using cassette mutagenesis and subcloned into *PCR2.1* plasmids (Invitrogen, Carlsbad, CA) by Lisa Klumb. The D128A protein was produced using the pET-21a/BL21(DE3) expression system (Novagen, Madison, WI) and refolded/purified as previously described.

DISSOCIATION KINETICS.

The off-rate of biotin from D128A was determined using a radiometric competition assay described previously in Chapter 2. Briefly, the protein was pre-loaded with a sub-stoichiometric concentration of 8,9-^{3}H-Biotin (Amersham, Arlington Heights, IL). Dissociation was initiated by the addition of a large excess of nonradioactive biotin. The amount of unbound radioactive biotin was determined over time by separation through spin-ultrafiltration and quantitation in a scintillation counter. The k_{off} was determined by fitting of the expression for a first order reaction. From the off-rates at each temperature, the transition-state enthalpy, $\Delta H^{\ddagger}$, and entropy, $\Delta S^{\ddagger}$ may be determined from a fit of the Eyring equation.

EQUILIBRIUM THERMODYNAMICS.

The relative binding affinity of D128A versus wild-type streptavidin was determined at 37 °C using a radiometric competition assay that has been previously described in Chapter 2. Briefly, in a mixture of 8,9-^{3}H-Biotin with histidine-tagged streptavidin (WT-Tag) and D128A, partitioning of the ^{3}H-Biotin to D128A may be determined by removing WT-Tag using Ni-NTA resin (Qiagen, Chatsworth, CA) and centrifugation before quantitation in a scintillation counter.

The binding enthalpies at 25 °C and 37 °C were determined using isothermal titration calorimetry on a CSC 4200 calorimeter (Calorimetry Sciences Corp. Provo, UT). Streptavidin solutions (30-40 μM) were titrated with 15-20 injections of biotin (250-750 μM, 5-10 μL per injection). All experiments were performed at pH 7 in 50 mM Na_2HPO_4 and 100 mM NaCl. The enthalpy of binding was extracted from the isotherm by non-linear least squares fitting to a model of independent binding sites using Dataworks™ from CSC and Igor Pro (Wavemetrics. Lake Oswego, OR).

X-RAY CRYSTALLOGRAPHY AND COMPUTER MODELING

Crystallographic analyses were performed by S. Freitag, I. LeTrong, and R.E. Stenkamp of the Biomolecular Structure Center. Potential of mean force molecular dynamics simulations of biotin dissociation were performed by J. Penzotti and T.P. Lybrand in the Department of Bioengineering. Methods for these analyses are described elsewhere.[100]

RESULTS

The D128A mutant displays a binding free energy decrease of 4.32 ± 0.04 kcal/mol relative to wild-type streptavidin at 37 °C (Table 6). This $\Delta\Delta G°$ is enthalpically driven, with a large +7.9 kcal/mol loss of binding enthalpy at 37 °C as determined by isothermal titration calorimetry. There is thus a significant reduction in the entropic costs of biotin association with the D128A mutant, with a calculated $T\Delta\Delta S°$ of + 3.6 kcal/mol relative to wild-type streptavidin at 37 °C. The dissociation rates were measured from 3-22 °C, which allowed the determination of a $\Delta H^{\ddagger}$ of +20.7 ± 1.1 kcal/mol for D128A relative to a $\Delta H^{\ddagger}$ of +30.4 ± 0.2 for wild-type streptavidin (Fig. 3). The extrapolated $\Delta G^{\ddagger}$ was 20.4 ± 1.6 kcal/mol at 37 °C versus 24.6 for wild-type streptavidin and the calculated $T\Delta S^{\ddagger}$ was 0.3 ± 1.2 kcal/mol versus 5.8 for wild-type streptavidin.

Table 6. Thermodynamic parameters for D128A at 37°C

Parameter	WT	D128A
K_a ratio (D128A:WT)	—	1032 ± 74
$\Delta\Delta G°$ (kcal/mol)	—	+4.3 ± 0.1
$\Delta\Delta H°$ (kcal/mol)	—	+7.9 ± 1.3
$T\Delta\Delta S°$ (kcal/mol)	—	+3.6 ± 1.3
ΔC_p (cal/mol·K)	-345	-238
k_{off} (10^{-6} /s)	29	28100
$\Delta G^{\ddagger}$ (kcal/mol)	+24.6 ± 0.2	+20.4 ± 2.3
$\Delta H^{\ddagger}$ (kcal/mol)	+30.4 ± 0.2	+20.7 ± 1.1
$T\Delta S^{\ddagger}$ (kcal/mol)	+5.8 ± 0.1	+0.3 ± 1.2

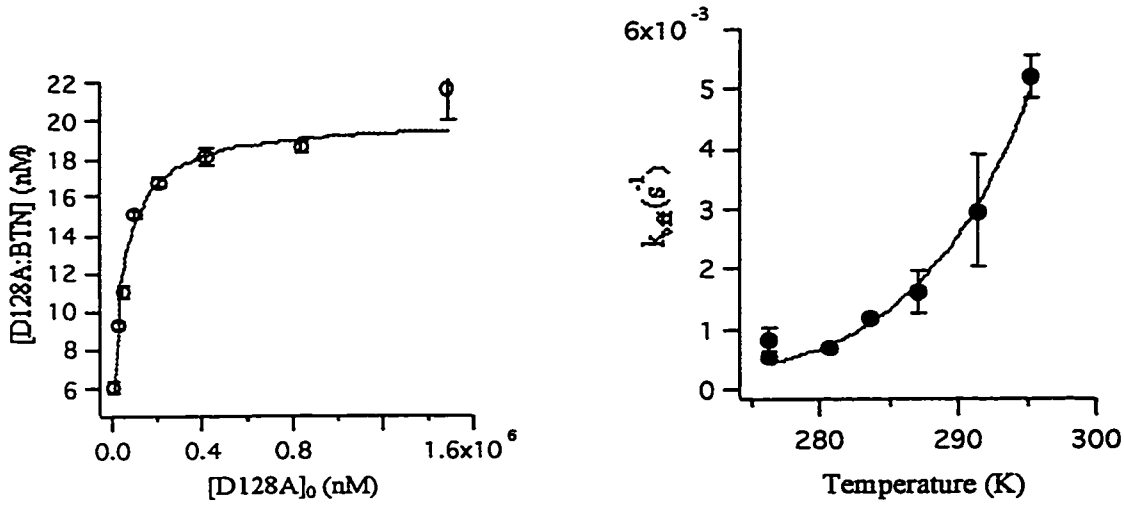

Figure 15. Equilibrium competition and Eyring transition state fits for D128A. Error bars denote one standard deviation.

DISCUSSION

The activation and thermodynamic parameters for the D128A mutant are consistent with those predicted for an intermediate that has traversed the early portion of the dissociation reaction coordinate through endothermic bond breaking and concomitant gain in configurational entropy. It had been previously hypothesized that the carboxylate bridging of the indole nitrogens of Trp 92 and Trp 108 serve to lessen the configurational entropy costs of biotin binding by immobilizing the side-chains in the unbound state. However, these residues appear to be fixed through packing interactions as the side-chains are not altered in the D128A mutant structure versus wild-type and also are similar in the bound and unbound states. The equilibrium entropy term is also more favorable in the mutant, consistent with a "looser" bound state.

The crystallographic structure of the D128A-biotin complex demonstrates that the thermodynamic and kinetic changes reflect a shift of biotin within the binding pocket away from the site of the mutation. Thus far, this is the first mutant of streptavidin in

which the position of biotin deviates from its usual location as seen in the WT complex. As a result, the enthalpic and entropic effects of the D128A mutation are hopelessly confounded by the additional effects of altered hydrogen bond lengths in the non-mutated residues of the binding site and wholesale movement of the three protein loops which delimit the binding site. Fortunately, the results of the PMF calculations allow us to interpret the biotin-bound structure in terms of intermediates along the biotin exit pathway.

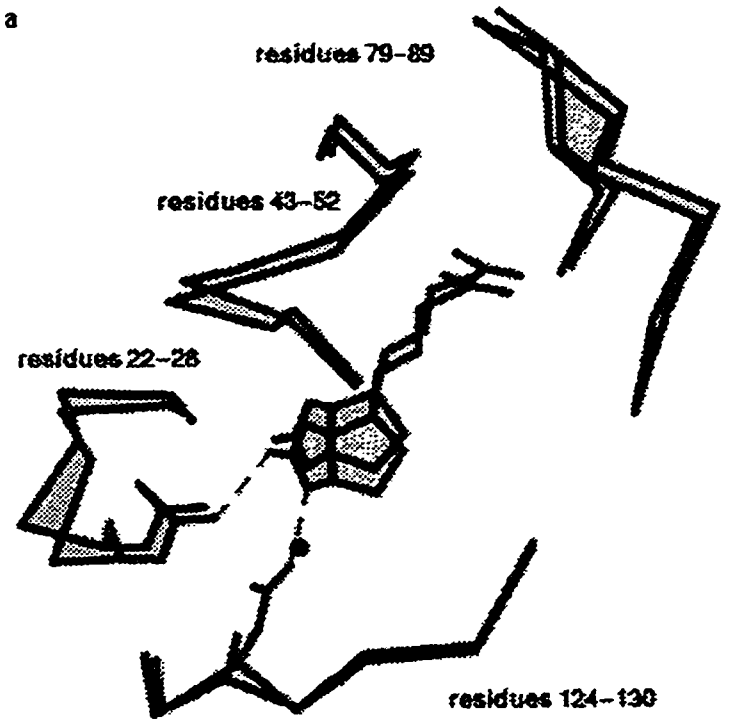

Figure 16. Superposition of the binding sites for WT and D128A complexes depicting the shift of biotin within the pocket and the concerted shift of surface loops away from the site of the D128A mutation.

In that context, Asp-128 appears to play a pivotal role in maintaining the equilibrium position of biotin in the hydrogen bond network of the binding pocket. The ground state destabilization is somewhat larger than might be predicted for a side-chain deletion given our previous experience with the residues that hydrogen bond to the ureido oxygen of biotin.[12] Preliminary results with an S45A mutant, however, support the potentially greater influence of the hydrogen bonds to the ureido nitrogens on the overall affinity.[101] The kinetic analysis of D128A suggests a lowered dissociation barrier in which enthalpic contacts have already been lost (vs. WT) and most of the entropic gain has already been realized. This is consistent with the picture of biotin becoming mobile and breaking bonds on its way out of the pocket toward a final, average transition state that, according to the changes in free energy, is identical in energy to the highest free energy barrier in WT also.

CONCLUSION

The composite structural, computational, and biophysical results suggest that biotin dissociates along a relatively well defined pathway. A striking property of the PMF calculations is the convergence of pathways in multiple dissociation simulations, where the same sequence of bond breaking and transient interactions is observed in nearly all simulations. Especially noteworthy is the early sequence where biotin slips out of the pocket as the Asn-23 bond is broken and a water molecule moves into the pocket to replace the lengthening Asp 128 carboxylate interaction with biotin. The D128A crystallographic structure displays a nearly identical movement of biotin, the accompanying Asn-23 bond breaking, and the presence of a water molecule that replaces the Asp-128 hydrogen bond to biotin. It is particularly interesting to compare these results with force microscopy measurements of the energetic landscape encountered upon pulling biotin out of the streptavidin pocket. A recent characterization of single biotin/streptavidin bonds under a wide range of loading rates suggested that the landscape consists of sharply defined barriers, again consistent with

a defined pathway.[102] Mechanistic molecular dynamics computations of the pathway for AFM experiments are also strikingly similar to our PMF calculations. Taken together, these results suggest that the biotin dissociation pathway in solution may be closely related to the pathway taken as biotin is pulled out of the pocket. This would perhaps be expected since the closest route of dissociation is along the direction where the carboxylate group of biotin exits the protein, the same point where biotin is tethered and thus pulled along in the force microscopy experiments. It thus appears that a reaction coordinate model of the activation landscape may be a useful representation of ligand dissociation from streptavidin, even with the complex set of molecular interactions that characterize the streptavidin-biotin complex. Finally, it is also intriguing that we may approximate an intermediate structure for a dissociating protein-ligand pair via site-directed mutagenesis. Perhaps by eliminating bonds in the correct order via this approach, we may obtain structures resembling intermediates even further out on the exit path.

CHAPTER 7: SUMMARY AND RECOMMENDATIONS

In this project, we have further investigated the origins of high-affinity binding in the streptavidin-biotin system to shed light on the general phenomenon of strong associations in protein-ligand pairs. In common with many such systems, the streptavidin-biotin pair relies on several motifs for generating a high-affinity interaction including hydrophobic interactions, hydrogen-bond networks, and movable protein segments. This document has focused on the latter two components and in particular on the D128 element of the hydrogen-bond networks and on the flexible loop at the binding site.

We have learned that the loop appears to retain biotin in the binding site by raising the barrier to dissociation. The mechanism by which the loop attains its ordered position in the biotin-bound complex remains unclear. What is apparent is that the N49 hydrogen bond to the biotin carboxylate is probably not responsible for nucleating loop closure since the residues at the loop edge achieve their "closed loop" conformation even in the absence of N49. We have also determined that creating a discontinuity in the loop impairs, but does not eliminate, its function. Nicking the loop highlights the management of entropic costs inherent in the involvement of mobile protein segments in ligand binding.

The remarkable resemblance of the D128A mutant to an intermediate complex seen in computer simulations of biotin dissociation led to the interpretation of the thermodynamic and kinetic results in terms of a reaction coordinate for dissociation rather than in terms of the role of a single hydrogen bond in the binding pocket. That a single mutation was able to produce this effect also emphasizes the importance of the D128 hydrogen bond to biotin.

Much of the analysis and interpretation in this document would have been impossible without the complementary structural information from X-ray crystallography studies. Clearly, a combined structural and thermodynamic approach to the investigation of high-affinity interactions is one of the most powerful tools available for dissecting the components of tight-binding pairs. This is especially important in light of the inability of current structural thermodynamic models to accurately predict binding behavior when expanded beyond the considerations of protein folding.

RECOMMENDATIONS

It remains to be seen whether the breakage of the S45—S52 hydrogen bond nucleated by the shift of the S45 side-chain causes the loop to close. This may become evident when the bound structure for the S45A mutant has been solved as retention of the A45—S52 bond in the bound state would argue strongly for that interpretation of the chain of events leading to loop closure. This would be a departure from previously seen mechanisms for movement of the binding site loop—charge negation, coupling to a deprotonation event,or natural motion of the protein.

Also, much more information about the role of the binding loop will become apparent when the structures for CP50/49 and CP49/48 are solved. It would be particularly exciting to see if the reduction in affinity is due to closure of only part of the loop. In a practical sense, evidence that the affinity of the streptavidin-biotin system could be modulated in a manner directly related to the number of loop residues could provide a method for creating a family of streptavidin mutants with differing affinities but otherwise consistent binding properties.

BIBLIOGRAPHY

1. Lindqvist, Y. and G. Schneider, *Protein-biotin interactions.* Current Opinion in Stuctural Biology, 1996. **6**: p. 798-803.

2. Green, N.M., *Avidin and Streptavidin.* Methods in Enzymology. Vol. 184. 1990: Academic Press, Inc. 51-67.

3. Sano, T., *et al., Molecular engineering of streptavidin.* Annals of the New York Academy of Sciences, 1996. **799**: p. 383-90.

4. Chilkoti, A., P.H. Tan, and P.S. Stayton, *Site-directed mutagenesis studies of the high-affinity steptavidin-biotin complex: Contributions of tryptophan residues 79, 108, and 120.* PNAS, 1995. **92**: p. 1754-1758.

5. Diamandis, E.P. and T.K. Christopoulos, *The biotin-(strept)avidin system: principles and applications in biotechnology.* Clinical Chemistry., 1991. **37**(5): p. 625-36.

6. Paganelli, G., M. Malcovati, and F. Fazio, *Monoclonal antibody pretargetting techniques for tumour localization: the avidin-biotin system. International Workshop on Techniques for Amplification of Tumour Targetting.* Nuclear Medicine Communications., 1991. **12**(3): p. 211-34.

7. Hnatowich, D.J., *The in vivo uses of streptavidin and biotin: a short progress report.* Nuclear Medicine Communications, 1994. **15**: p. 575-577.

8. Stayton, P.S., *et al., Control of protein-ligand recognition using a stimuli-responsive polymer.* Nature, 1995. **378**: p. 472-474.

9. Koppenol, S. and P.S. Stayton, *Engineering two-dimensional protein order at surfaces.* J Pharm Sci, 1997. **86**(11): p. 1204-9.

10. Chilkoti, A. and P.S. Stayton, *Molecular Origins of the Slow Streptavidin-Biotin Dissociation Kinetics.* Journal of the American Chemical Society, 1995. **117**: p. 10622-10628.

11. Freitag, S., *et al., Structural studies of binding site tryptophan mutants in the high- affinity streptavidin-biotin complex.* J Mol Biol, 1998. **279**(1): p. 211-21.

12. Klumb, L.A., V. Chu, and P.S. Stayton, *Energetic roles of hydrogen bonds at the ureido oxygen binding pocket in the streptavidin-biotin complex.* Biochemistry, 1998. **37**(21): p. 7657-63.

13. Weber, P.C., *et al., Structural Origins of High-Affinity Biotin Binding to Streptavidin.* Science, 1989. **243**: p. 85-88.

14. Freitag, S., *et al., Structural studies of the streptavidin binding loop.* Protein Sci, 1997. **6**(6): p. 1157-66.

15. Chu, V., *et al., Thermodynamic and structural consequences of flexible loop deletion by circular permutation in the streptavidin-biotin system.* Protein Science, 1998. 7(4): p. 848-59.

16. Hendrickson, W.A., *et al., Crystal structure of core streptavidin determined from multiwavelength anomalous diffraction of synchrotron radiation.* Proceedings of the National Academy of Sciences USA, 1989. **86**: p. 2190-2194.

17. Weber, P., *et al., Crystallographic Data for Streptomyces avidinii Streptavidin.* Journal of Biological Chemistry, 1987. **262**(26): p. 12728-12729.

18. Pähler, A., *et al., Characterization and Crystallization of Core Streptavidin.* Journal of Biological Chemistry, 1987. **262**(29): p. 13933-13937.

19. Weber, P.C., *et al., Crystallographic and Thermodynamic Comparison of Natural and Synthetic Ligands Bound to Streptavidin.* Journal of the American Chemical Society, 1992. **114**: p. 3197-3200.

20. Weber, P.C., M.W. Pantoliano, and L.D. Thompson, *Crystal structure and ligand-binding studies of a screened peptide complexed with streptavidin.* Biochemistry, 1992. **31**: p. 9350-9354.

21. Weber, P.C., *et al., Structure-based design of sythetic azobenzene ligands for streptavidin.* Journal of the American Chemical Society, 1992. **114**: p. 3197-3200.

22. Katz, B.A., *Binding to protein targets of peptidic leads discovered by phage display: cyrstal structures of streptavidin-bound linear and cyclic peptide ligands containing the HPQ sequence.* Biochemistry, 1995. **34**: p. 15421-15429.

23. Katz, B.A., B. Liu, and R. Cass, *Structure-based design tools: structural and thermodynamic comparison with biotin of a small molecule that binds to streptavidin with micromolar affinity.* Journal of the American Chemical Society, 1996. **118**: p. 7914–7920.

24. Schmidt, T.G.M., *et al., Molecular interaction between the strep-tag affinity peptide and its cognate target, streptavidin.* Journal of Molecular Biology, 1996. **255**: p. 753-766.

25. Athappilly, F.K. and W.A. Hendrickson, *Crystallographic analysis of the pH-dependent binding of iminobiotin by streptavidin.* Protein Science, 1997. **6**: p. 1338–1342.

26. Sano, T., C.L. Smith, and C.R. Cantor, *A streptavidin mutant containing a cysteine stretch that facilitates production of a variety of specific streptavidin conjugates.* Bio/Technology., 1993. **11**(2): p. 201-6.

27. Sano, T. and C.R. Cantor, *Intersubunit contacts made by tryptophan 120 with biotin are essential for both strong biotin binding and biotin-induced tighter subunit association of streptavidin.* Proceedings of the National Academy of Sciences USA, 1995. **92**: p. 3180-3184.

28. Sano, T. and C.R. Cantor, *Intersubunit contacts made by tryptophan 120 with biotin are essential for both strong biotin binding and biotin-induced tighter subunit association of streptavidin.* Proceedings Of the National Academy Of Sciences Of the United States Of America., 1995. **92**(8): p. 3180-4.

29. Miyamoto, S. and P.A. Kollman, *Absolute and relative binding free energy calculations of the interaction of biotin and its analogs with streptavidin using molecular dynamics/free energy perturbation approaches.* Proteins., 1993. **16**(3): p. 226-45.

30. Moy, V.T., E.L. Florin, and H.E. Gaub, *Intermolecular forces and energies between ligands and receptors.* Science., 1994. **266**(5183): p. 257-9.

31. Chilkoti, A., *et al.*, *The relationship between ligand-binding thermodynamics and protein-ligand interaction forces measured by atomic force microscopy.* Biophysical Journal., 1995. **69**(5): p. 2125-30.

32. Grubmüller, H., B. Heymann, and P. Tavan, *Ligand Binding: Molecular Mechanics Calculation of the Streptavidin-Biotin Rupture Force.* Science, 1996. **271**: p. 997-999.

33. Kempner, E.S., *Movable lobes and flexible loops in proteins. Structural deformations that control biochemical activity.* Febs Letters., 1993. **326**(1-3): p. 4-10.

34. Derreumaux, P. and T. Schlick, *The loop opening/closing motion of the enzyme triosephosphate isomerase.* Biophysical Journal, 1998. **74**: p. 72–81.

35. Sampson, N.S. and J.R. Knowles, *Segmental motion in catalysis: Investigation of a hydrogen bond critical for loop closure in the reaction of triosphosphate isomerase.* Biochemistry, 1992. **31**: p. 8488–8494.

36. Sampson, N.S. and J.R. Knowles, *Segmental movement: Definition of the structural requirements for loop closure in catalysis by triosephosphate isomerase.* Biochemistry, 1992. **31**: p. 8482–8487.

37. Pompliano, D.L., A. Peyman, and J.R. Knowles, *Stabilization of a reaction intermediate as a catalytic device: Definition of the functional role of the flexible loop in triosphosphate isomerase.* Biochemistry, 1990. **29**: p. 3186-3194.

38. Wierenga, R.K., *et al.*, *The crystal structure of the "open" and the "closed" conformation of the flexible loop of trypanosomal triosephosphate isomerase.* Proteins: Structure, Function, and Genetics, 1991. **10**: p. 33–49.

39. Noble, M.E.M., J.P. Zeelen, and R.K. Wierenga, *Structures of the "open" and "closed" state of trypanosomal triosephosphate isomerase, as observed in a new crystal form: implications for the reaction mechanism.* Proteins: Structure, Function, and Genetics, 1993. **16**: p. 311-326.

40. Zhang, Z., *et al.*, *Crystal structure of recombinant chicken triosephosphate isomerase-phosphoglycolohydroxamate complex at 1.8-Å resolution.* Biochemistry, 1994. **33**: p. 2830–2837.

41. Williams, J.C. and A.E. McDermott, *Dynamics of the flexible loop of triosephosphate isomerase: The loop motion is not ligand gated.* Biochemistry, 1995. **34**: p. 8309–8319.

42. Gerstein, M. and C. Chothia, *Analysis of protein looop closure. Two types of hinges produce one motion in lactate dehydrogenase.* Journal of Molecular Biology, 1991. **220**: p. 133–149.

43. Clarke, A.R., *et al.*, *Site-directed mutagenesis reveals role of mobile arginine residue in lactate dehydrogenase catalysis.* Nature, 1986. **324**(18): p. 699–702.

44. Fry, D.C., S.A. Kuby, and A.S. Midlvan, *ATP-binding site of adenylate kinase: mechanistic implications of its homology with ras-encoded p21, F_1-ATPase, and other nucleotide-binding proteins.* PNAS, 1986. **83**: p. 907-911.

45. Larson, E.M., F.W. Larimer, and F.C. Hartman, *Mechanistic insights provided by deletion of a flexible loop at the active site of ribulose-1,5-bisphosphate carboxylase/oxygenase.* Biochemistry, 1995. **34**: p. 4531–4537.

46. Tanaka, T., *et al.*, *Mutational and Proteolytic Studies on a Flexible Loop in Glutathione Synthetase from Escherichia coli B: The Loop and Arginine 233 Are Critical for the Catalytic Reaction.* Biochemistry, 1992. **31**: p. 2259-2265.

47. Bystroff, C. and J. Kraut, *Crystal structure of unliganded Escherichia coli dihydrofolate reductase. Ligand-induced conformational changes and cooperativity in binding.* Biochemistry, 1991. **30**: p. 2227–2239.

48. Falzone, C.J., P.E. Wright, and S.J. Benkovic, *Dynamics of a flexible loop in dihydrofolate reductase from Escherichia coli and its implication for catalysis.* Biochemistry, 1994. 33(2): p. 439-442.

49. Tanaka, T., T. Nishioka, and J.i. Oda, *Nicked multifunctional loop of glutathione synthetase still protects the catalytic intermediate.* Archives of Biochemistry and Biophysics, 1997. **339**(1): p. 151–156.

50. Landry, S.J., *et al.*, *Interplay of structure and disorder in cochaperonin mobile loops.* Proceedings of the National Academy of Sciences, USA, 1996. **93**: p. 11622–11627.

51. Murphy, K.P., *et al., Structural Energetics of Peptide Recognition: Angiotensin II/Antibody Binding.* Proteins: Structure, Function , and Genetics, 1993. **15**: p. 113-120.

52. Spolar, R.S. and M.T. Record, Jr., *Coupling of local folding to site-specific binding of proteins to DNA.* Science, 1994. **263**: p. 777-784.

53. Thornton, J.M. and B.L. Sibanda, *Amino and Carboxy-terminal Regions in Globular Proteins.* Journal of Molecular Biology, 1983. **167**: p. 443-460.

54. Carrington, D.M., A. Auffret, and D.E. Hanke, *Polypeptide ligation occurs during post-tranlational modification of concanavalin A.* Nature, 1985. **313**: p. 64-67.

55. Cunningham, B.A., *et al., Favin versus concanavalin A: cicularly permuted amino acid sequences.* PNAS, 1979. **76**(7): p. 3218-3222.

56. Einspahr, H., *et al., The crystal structure of pea lectin at 3.0-Å resolution.* Journal of Biological Chemistry, 1986. **261**(35): p. 16518-16527.

57. Reeke, G.N., Jr. and J.W. Becker, *Three-dimensional structure of favin: saccharide binding-cyclic permutation in leguminous lectins.* Science, 1986. **234**(4780): p. 1108-11.

58. Hardman, K.D. and C.F. Ainsworth, *Structure of concanavalin A at 2.4-Å resolution.* Biochemistry, 1972. **11**(26): p. 4910-4919.

59. Meehan, E.J., Jr., *et al., The crystal structure of pea lectin at 6-Å resolution.* Journal of Biological Chemistry, 1982. **257**(22): p. 13278–13282.

60. Goldenberg, D.P. and T.E. Creighton, *Circular and circularly permuted forms of bovine pancreatic trypsin inhibitor.* Journal of Molecular Biology, 1983. **165**: p. 407-413.

61. Luger, K., *et al., Correct folding of circularly permuted variants of a βα barrel enzyme in vivo.* Science, 1989. **243**: p. 206-209.

62. Heinemann, U. and M. Hahn, *Circular permutation of polypeptide chains: implications for protein folding and stability.* Prog. Biophys. Molec. Biol., 1995. **64**(2/3): p. 121-143.

63. Komar, A.A. and R. Jaenicke, *Kinetics of translation of γB crystallin and its circularly permutated variant in an in vitro cell-free system: possible relations to codon distribution and protein folding.* FEBS Letters, 1995. **376**: p. 195-198.

64. Koebnik, R. and L. Krämer, *Membrane assembly of circularly permuted variants of the E. coli outer membrane protein OmpA.* Journal of Molecular Biology, 1995. **250**: p. 617-626.

65. Schachman, H.K., *Formation of Active Enzyme from Polypeptide Fragments and Circularly Permutated Chains: Model Studies with Aspartate Transcarbamoylase*, . 1994.

66. Kreitman, R.J., R.K. Puri, and I. Pastan, *A circularly permuted recombinant interleukin 4 toxin with increased activity.* PNAS USA, 1994. **91**: p. 6889-6893.

67. Hofmann, K., *et al.*, *Iminobiotin affinity columns and their application to retrieval of streptavidin.* PNAS, 1980. **8**: p. 4666-4668.

68. Sano, T. and C.R. Cantor, *Expression of a cloned streptavidin gene in Escherichia coli.* Proceedings of the National Academy of Sciences USA, 1990. **87**: p. 142-146.

69. Pace, C.N., *et al.*, *How to measure and predict the molar absorption coefficient of a protein.* Protein Science, 1995. **4**: p. 2411-2423.

70. Freire, E., O.L. Mayorga, and M. Straume, *Isothermal Titration Calorimetry.* Analytical Chemistry, 1990. **62**(18): p. 950A-959A.

71. Piran, U. and W.J. Riordan, *Dissociation rate constant of the biotin-streptavidin complex.* Journal of Immunological Methods, 1990. **133**: p. 141-143.

72. Hahn, M., *et al.*, *Native-like in vivo folding of a circularly permuted jellyroll protein shown by crystal structure analysis.* PNAS USA, 1994. **91**: p. 10417-10421.

73. Viguera, A.R., L. Serrano, and M. Wilmanns, *Different folding transition states may result in the smae native structure.* Nature Structural Biology, 1996. 3(10): p. 874-880.

74. Pieper, U., *et al.*, *Circularly permuted β-lactamase from Staphylococcus aureus PC1.* Biochemistry, 1997. **36**: p. 8767–8774.

75. Horlick, R.A., *et al.*, *Permuteins of interleukin 1β—a simplified approach for the construction of permutated proteins having new termini.* Protein Engineering, 1992. 5(5): p. 427-431.

76. Freire, E., I. Luque, and B. Townsend, *ASAcalc: Calculation of accessible surface areas*, . 1997, Biocalorimetry Center: The Johns Hopkins University: Baltimore.

77. Sano, T. and C.R. Cantor, *Expression Vectors for Streptavidin-Containing Chimeric Proteins.* Biochemical and Biophysical Research Communications, 1991. **176**(2): p. 571-577.

78. Ben-Bassat, A., *Methods for removing N-terminal methionine from recombinant proteins.* Bioprocess Technology, 1991. **12**: p. 147-159.

79. Freire, E., *Structural thermodynamics: Prediction of protein stability and protein binding affinities.* Archives of Biochemistry and Biophysics, 1993. **303**(2): p. 181–184.

80. Connolly, M.L., *Solvent-accessible surfaces of proteins and nucleic acids.* Science, 1983. **221**(4612): p. 709-713.

81. Lee, B. and F.M. Richards, *The interpretation of protein structures: estimation of static accessibility.* Journal of Molecular Biology, 1971. **55**: p. 379-400.

82. Jorgensen, W.L., J. Gao, and C. Ravimohan, *Monte carlo simulations of alkanes in water: Hydration numbers and the hydrophobic effect.* Journal of Physical Chemistry, 1985. **89**: p. 3470–3473.

83. Hermann, R.B., *Theory of hydrophobic bonding. II. The correlation of hydrocarbon solubility in water with solvent cavity surface area.* The Journal of Physical Chemistry, 1972. **76**(19): p. 2754-2759.

84. Shrake, A. and J.A. Rupley, *Environment and exposure to solvent of protein atoms. Lysozyme and insulin.* Journal of Molecular Biology, 1973. **79**: p. 351-371.

85. Richmond, T.J., *Solvent accessible surface area and excluded volume in proteins.* Journal of Molecular Biology, 1984. **178**: p. 63-89.

86. Gill, S.J. and I. Wadsö, *An equation of state describing hydrophobic interactions.* Proceedings of the National Academy of Sciences, USA, 1976. **73**(9): p. 2955-2958.

87. Livingstone, J.R., R.S. Spolar, and J. M. Thomas Record, *Contribution to the thermodynamics of protein folding from the reduction in water-accessible nonpolar surface area.* Biochemistry, 1991. **30**: p. 4237-4244.

88. Sturtevant, J.M., *Heat capacity and entropy changes in processes involving proteins.* PNAS, 1977. **74**(6).

89. Murphy, K.P. and S.J. Gill, *Solid model compounds and the thermodynamics of protein unfolding.* Journal of Molecular Biology, 1991. **222**: p. 699-709.

90. Gómez, J., *et al.*, *The heat capacity of proteins.* Proteins: Structure, Function, and Genetics, 1995. **22**: p. 404-412.

91. Bains, G., *et al.*, *Microcalorimetric study of wheat germ agglutinin binding to N-acetylglucosamine and its oligomers.* Biochemistry, 1992. **31**: p. 12624–12628.

92. McNemar, C., *et al.*, *Thermodynamic and structural analysis of phosphotyrosine polypeptide binding to Grb2-SH2.* Biochemistry, 1997. **36**: p. 10006–10014.

93. Hibbits, K.A., D.S. Gill, and R.C. Willson, *Isothermal titration calorimetric study of the association of hen egg lysozyme and the anti-lysozyme antibody HyHEL-5.* Biochemistry, 1994. **33**: p. 3684-3590.

94. Gómez, J. and E. Freire, *Thermodynamic mapping o the inhibitor site of the aspartic protease endothiapepsin.* Journal of Molecular Biology, 1995. **252**: p. 337–350.

95. Connelly, P.R. and J.A. Thomson, *Heat capacity changes and hydrophobic interactions in the binding of FK506 and rapamycin to the FK 506 binding protein.* PNAS, 1992. **89**: p. 4781-4785.

96. Schwarz, F.P., *et al.*, *Thermodynamics of antigen-antibody binding using specific anti-lysozyme antibodies.* European Journal of Biochemistry, 1995. **228**: p. 388-394.

97. Raman, C.S., M.J. Allen, and B.T. Nall, *Enthalpy of antibody-cytochrome c binding.* Biochemistry, 1995. **34**: p. 5831–5838.

98. Pearce, K.H., Jr., *et al.*, *Structural and mutational analysis of affinity-inert contact residues at the growth hormone-receptor interface.* Biochemistry, 1996(35): p. 10300–10307.

99. Frisch, C., *et al.*, *Thermodynamics of the interaction of barnase and barstart: Changes in free energy versus changes in enthalpy on mutation.* Journal of Molecular Biology, 1997. **267**: p. 696–706.

100. Freitag, S., *et al.*, *A structural snapshot of an intermediate on the streptavidin-biotin dissociation pathway.* In review.

101. Hyre, D., *Personal communication*, . 1998.

102. Evans, E. and K. Ritchie, *Dynamic strength of molecular adhesion bonds.* Biophys J, 1997. **72**(4): p. 1541-55.

APPENDIX A: STRUCTURAL THERMODYNAMICS DATABASES

Protein databases used for parameterizations in structural thermodynamic studies.

Database used by Livingstone, Spolar, and Record	Database used by Freire
α-Chymotrypsin	Chymotrypsin
β-Trypsin	Trypsin
Carbonic Anhydrase	Carbonic Anhydrase
Chymotrypsinogen	Protein G
Ferricytochrome	Cytochrome C
Lysozyme	Lysozyme
Metmyoglobin	Myoglobin
Papain	Papain
Parvalbumin B	Parvalbumin
Pepsinogen	Pepsinogen
Ribonuclease A	Ribonuclease A
Ribonuclease T1	Ribonuclease T1
Staph. Nuclease	Staph. Nuclease
Trypsin Inhibitor	α-Lactalbumin

APPENDIX B: BINDING SITE RESIDUES IN STREPTAVIDIN

These residues were used in the ΔASA calculations localized to the binding sites of WT and CP51/46 in Chapter 5.

Asparagine-23	Alanine-50
Glutamine-24	Glutamate-51
Leucine-25	Serine-52
Glycine-26	Tryptophan-79
Serine-27	Serine-88
Tyrosine-43	Threonine-90
Serine-45	Tryptophan-92
Alanine-46	Tryptophan-108
Valine-47	Tryptophan-120
Glycine-48	Aspartate-128
Asparagine-49	

APPENDIX C: ITC DATA, CP49/48 AND CP50/49

These are overall results for fitting of multiple, independent binding site models to the ITC data of CP49/48 and CP50/49. Where available, I have reported the standard deviations for the fitting parameter values:

1. **n**: Number of binding sites. Since concentrations are expressed in μM of subunits, this value should be approximately 1.0.
2. K_a: Affinity constant. Expressed in M^{-1}.
3. $\Delta H°$: Enthalpy of binding. Expressed in kcal/mol

CP49/48

Temperature	Data File	Conc.	n:	sd n	Ka	sd Ka	ΔH	sd ΔH	RMS	Chi-square	Buffer	Date:	Reject
10	CP49 10A		0.8169	0.002	1.03E+08	1.70E+07	-16.20	0.09		27	PB	10/1/98	
10	CP49 10B		0.7978	0.0024	8.41E+07	1.42E+07	-16.58	0.11		41	PB	10/2/98	
25	CP49 25A										PB	10/13/98	x
25	CP49 25B		0.7612	1.1888			-17.88	0.3		21	PB	10/14/98	
25	CP49 25C		0.8401	0.001	2.50E+08	9.30E+07	-19.15	0.07		58	PB	10/15/98	
25	CP49 25D		0.8351	0.0013	1.56E+08	2.70E+07	-19.82	0.07		17	PB	10/23/98	
37	CP49 37A		0.8967	0.0022			-20.36	0.12		39	PB	10/20/98	
37	CP49 37B		0.8914	0.0021			-21.00	0.12		15	PB	10/21/98	
10	CP49R10A										PB	12/1/98	
25	CP49R25A		0.9957	0.0049	8.72E+07		-18.59	0.26		9	PB	11/28/98	
37	CP49R37A		1.0014	0.0029	1.55E+08	1.09E+08	-18.74	0.16		14	PB	11/30/98	
25	CP49T25A		0.8858	0.0025	1.79E+10	1.37E+10	-16.70	0.1		34	Tris	9/6/98	
25	CP49T25B		0.8695	0.0016	2.13E+08	1.33E+08	-17.30	0.1		48	Tris	9/7/98	
25	CP49T25C		0.984	0.0018	1.99E+08	4.90E+07	-20.60	0.14		99	Tris	9/8/98	
25	CP49T25D		0.6076	0.0023	5.08E+08	5.06E+08	-20.63	0.18		17	Tris	9/17/98	x
37	CP49T37A		0.6238	0.0024	7.69E+08	1.30E+09	-23.97	0.23		48	Tris	9/20/98	x
37	CP49T37B		0.6257	0.0037	2.63E+08	1.05E+09	-22.06	0.33		9	Tris	9/20/98	x
37	CP49T37C		0.6738	0.0723	1.13E+08	1.26E+08	-24.58	0.23		15	Tris	9/21/98	x

CP50/49

Temperature	Data File	Conc.	n:	sd n	Ka	sd Ka	ΔH	sd ΔH	RMS	Chi-square	Buffer	Date:	Reject
10	CP50 10A		0.7912	0.0019	1.41E+08	5.70E+07	-17.37	0.11		29	PB	9/28/98	
10	CP50 10B		0.8162	0.0009	2.58E+08	9.80E+07	-16.99	0.05		51	PB	9/30/98	
10	CP50 10C		0.8136	0.0029	1.16E+08	6.90E+07	-17.31	0.16		175	PB	9/30/98	
25	CP50 25A		0.8519	0.0012	9.94E+07	1.08E+07	-18.59	0.06		68	PB	6/19/98	
25	CP50 25C		0.8898	0.001	4.09E+08	2.70E+08	-19.06	0.07		18	PB	7/2/98	
37	CP50 37A		0.8477	0.003	1.78E+08	1.34E+08	-20.73	0.11		102	PB	6/27/98	
37	CP50 37B		0.8536	0.0018	1.47E+08	2.70E+07	-21.26	0.11		23	PB	6/28/98	
10	CP50R10A		0.9417	0.0027	1.62E+08	5.40E+07	-15.97	0.11		21	PB	12/3/98	
25	CP50R25A		0.8827	0.0014	2.89E+08	2.20E+08	-19.13	0.08		88	PB	11/27/98	
37	CP50R37A		0.9917	0.0008	1.29E+08	1.70E+07	-20.78	0.05		82	PB	12/2/98	
25	CP50T25A		0.7372	0.0031	2.46E+08	5.52E+08	-18.84	0.15		14	Tris	7/4/98	
25	CP50T25B		0.7664	0.0033	1.94E+08	1.62E+08	-17.04	0.19		8	Tris	7/28/98	
25	CP50T25C											9/4/98	x
25	CP50T25D		0.7395	0.0011	2.10E+08	6.70E+07	-19.97	0.1		62	Tris	9/5/98	
25	CP50T25E		0.673	0.0023	7.32E+07	2.56E+07	-17.59	0.14		40	Tris	9/12/98	x

APPENDIX D: ITC DATA, CP51/46 AND D128A

These are overall results for fitting of multiple, independent binding site models to the ITC data of CP51/46 and D128A. Where available, I have reported the standard deviations for the fitting parameter values:

1. **n**: Number of binding sites. Since concentrations are expressed in μM of subunits, this value should be approximately 1.0.
2. K_a: Affinity constant. Expressed in M^{-1}.
3. $\Delta H°$: Enthalpy of binding. Expressed in kcal/mol

CP51/46

Temperature	Data File	Conc.	n:	sd n	Ka	sd Ka	ΔH	sd ΔH	RMS	Chi-square	Buffer	Date:	Reject
10	cp10a	34.4	0.8605		1.64E+07		-12.37		24.88		Phos	12/12/96	
10	cp10b	34.4	0.9275		2.22E+07		-12.00		21.19		Phos		
10	cp10c	34.4	0.9255		4.03E+07		-11.80		34.3		Phos	4/18/97	
10	cp10d	37.2									Phos	3/26/97	x
10	cp10e	32.3	0.8715		4.99E+07		-11.89		25.89		Phos	4/16/97	
10	cp10f	32.3	0.7853		1.75E+07		-13.52		25.38		Phos		
10	cp10g	32.3	0.7837		1.74E+07		-13.23		46.06		Phos		
25	cp25B	34.4	0.9606		1.29E+07		-12.69		13.44		Phos		
25	cp25C	34.4	0.9368		3.81E+07		-11.38		9.46		Phos		
25	cp25D	34.4	0.9148		3.31E+07		-12.72		24.07		Phos		
25	cp25d	31.2									Phos		x
25	cp25e	31.2									Phos		x
25	cp25f	31.2	0.89		2.50E+07		-13.20		18.09		Phos	3/18/97	
25	cp25g	37.2	0.94		1.73E+07		-14.48		32.65		Phos		
25	cp25h	37.2	0.96		2.12E+07		-13.96		30.41		Phos		
25	cp25i	37.2	0.9291		1.86E+07		-14.60		16.53		Phos	4/3/97	
25	cp25j	37.2	0.9329		2.77E+07		-13.85		45.64		Phos	4/4/97	
25	cp25k	37.2	0.98		2.72E+07		-12.59		49.15		Phos	4/8/97	
25	cp25l	34.5	0.8636		6.79E+06		-15.39				Phos	4/20/97	x
25	cp25m	34.5	0.8503		1.06E+07		-15.06		56.77		Phos	4/21/97	x
37	cp37a	34.4	0.8547		5.71E+06		-16.01		21.84		Phos		
37	cp37b	34.4	0.9197		4.18E+06		-17.11		92.73		Phos		
37	cp37c	34.4	0.9171		6.50E+06		-16.63		95.43		Phos		
37	cp37d	31.2	1.0076		2.40E+09		-16.27				Phos		x
37	cp37e	37.2	0.96		1.02E+07		-14.89		33.42		Phos		
37	cp37f	37.2	0.9		7.72E+06		-15.27		30.96		Phos		
25	cp25/tris1	10.7	1.0607		4.44E+07		-11.64				Tris		
25	cp25/tris2	10.7	0.9822		3.22E+07		-11.41				Tris		
25	tcp25a	31.6	0.8584		1.97E+07		-13.41		16.53		Tris	4/25/97	
25	tcp25b	31.6	0.8747		4.54E+07		-12.75		32.53		Tris		
25	tcp25c	31.6	0.8448		9.00E+06		-14.10		68.63		Tris	4/28/97	

D128A

Temperature	Data File	Conc.	n:	sd n	Ka	sd Ka	ΔH	sd ΔH	RMS	Chi-square	Buffer	Date:	Reject
37	D128A37A	28.8	0.851		2.15E+16		-21.70				Phos	11/16/97	
37	D128A37B	28.8	0.8086	0.0044	8.98E+08	3.40E+07	-21.80	0.3		14	Phos	11/28/97	
37	D128A37C	28.8	0.9093	0.0021	2.69E+07	3.12E+08	-21.50	0.1		59	Phos	12/22/97	
25	D128A25A	13.8	0.8484	0.0024	2.48E+09	9.40E+08	-18.78	0.15		204	Phos		
25	D128A25B	13.8	0.8907	0.006	1.90E+08	8.70E+07	-18.37	0.3		7	Phos		

VANO CHU

8618 17th Ave Northeast
Seattle, Washington 98115
206-523-0439

EDUCATION

1991–1998 **University of Washington.** Seattle, Washington.
Department of Bioengineering.
Ph.D., Bioengineering.
Dissertation: Molecular Recognition in the Streptavidin-Biotin System.
Whitaker Foundation Fellow, 1992–1997.

1987–1991 **University of Florida.** Gainesville, Florida.
Department of Material Science and Engineering.
Bachelor of Science in Engineering (MSE).
Minor in Business Administration.
Valedictorian. National Merit Corporate Scholar, 1987–1991.

RESEARCH EXPERIENCE

1994–1998 **University of Washington. Seattle, Washington.**
Department of Bioengineering.
Doctoral Candidate, Laboratory of Professor Patrick Stayton.
Investigation of the biophysics of streptavidin-biotin interaction through circular permutation and site-directed mutagenesis. Modification of single-chain antibodies for improved solubility and introduction of chemical conjugation sites. Collaboration with Biomolecular Structure Center for crystallographic and structural thermodynamic analyses of streptavidin mutants. Collaboration with Departments of Urology and Radiation Oncology for *in vivo* evaluation of single-chain antibody mutants.

1991–1994 **University of Washington. Seattle, Washington.**
Department of Bioengineering.
Doctoral Candidate, Laboratory of Professor Christopher Viney.
Characterization of liquid-crystalline polysiloxanes for dental implant applications using polarized light-microscopy and differential scanning calorimetry. Investigation of the origins of liquid-crystallinity in tolane oligomers. Study of biomineralization in diatoms using light-microscopy and scanning- and transmission-electron microscopy.

1990–1991 **University of Florida. Gainesville, Florida.**
Department of Materials Science and Engineering.
Undergraduate Assistant, Laboratory of Professor Eugene Goldberg.
Modification of polyvinyl chloride tubing with radiation-polymerized *N*-vinyl pyrrolidone/polymethylmethacrylate coatings for blood transport applications.

Summer 1990 **Dow Chemical Corporation. Freeport, Texas.**
Analytical & Engineering Sciences.
Summer Intern. Supervisor: Lorraine M. Kroposki.
Fatigue testing of polymeric materials for automotive applications. Characterization of failure modes and fracture surfaces through photmicrography and video-capture analysis.

PUBLICATIONS

Protein Engineering

S. Frietag, V. Chu, J.E. Penzotti, L.A. Klumb, R. To, I. LeTrong, T.P. Lybrand, R.E. Stenkamp, and P.S. Stayton. "A structural snapshot of an intermediate on the streptavidin-biotin dissociation pathway." Submitted for review.

P. Tan, V. Chu, J. Stray, D. Hamlin, D. Petit, S.D. Wilbur, R.L. Vessella, and P.S. Stayton. "Engineering the isoelectric point of a renal cell carcinoma targeting antibody greatly enhances scFv solubility." *Immunotechnology*. Accepted for publication.

V. Chu, S. Freitag, I. LeTrong, R. Stenkamp, and P.S. Stayton. "Thermodynamic and structural consequences of flexible loop deletion by circular permutation in the streptavidin-biotin system." *Protein Science*. **7**: 848–859. (1998)

L.A. Klumb, V. Chu, and P.S. Stayton. "Energetic roles of hydrogen bonds at the ureido oxygen binding pocket in the streptavidin-biotin complex." *Biochemistry*. **37**: 7657–7663. (1998)

A. Chilkoti, V. Chu, L.A. Klumb, and P.S. Stayton. "Molecular origins of the slow streptavidin-biotin dissociation kinetics." *34th Hanford Symposium on Health and the Environment. Biomacromolecules: From 3-D Structure to Applications*. Poster. (1995)

Liquid Crystals

R.J. Twieg, V. Chu, C. Nguyen, C.M. Dannels, and C. Viney. "Tolane oligomers: Model thermotropic liquid crystals." *Liquid Crystals*. **20**: 287–292. (1996)

P. Nguyen, G. Lesley, C. Dai, N.J. Taylor, T.B. Marder, V. Chu, C. Viney, I. Ledoux, and J. Zyss. "Well-defined conjugated rigid-rods as multifunctional materials: Linear and nonlinear optical properties and liquid crystalline behavior," in J.F. Harrod and R.M. Laine, eds. *Applications of organometallic chemistry in the preparation and processing of advanced materials*. Kluwer Academic Publishers: Dordrect, pp. 333–347. (1995)

A. Sellinger, R.M. Laine, V. Chu, and C. Viney. "Palladium- and platinum-catalyzed coupling reactions fo allyoxy aromatics with hydridosilanes and hydridosiloxanes: Novel liquid crystalline organosilane materials." *Journal of Polymer Science: Part A: Polymer Chemistry*. **32**: 3069–3089. (1994)